NAVAL POSTGRADUATE SCHOOL

MONTEREY, CALIFORNIA

THESIS

SIMULATION OF WIRELESS PROPAGATION AND JAMMING IN A HIGH-RISE BUILDING

by

Yildirim Kaya

September 2005

Thesis Advisor:	David C. Jenn
Second Reader:	Daniel C. Schleher

REPORT DOCUMENTATION PAGE			*Form Approved OMB No. 0704-0188*
Public reporting burden for this collection of information is estimated to average 1 hour per response, including the time for reviewing instruction, searching existing data sources, gathering and maintaining the data needed, and completing and reviewing the collection of information. Send comments regarding this burden estimate or any other aspect of this collection of information, including suggestions for reducing this burden, to Washington headquarters Services, Directorate for Information Operations and Reports, 1215 Jefferson Davis Highway, Suite 1204, Arlington, VA 22202-4302, and to the Office of Management and Budget, Paperwork Reduction Project (0704-0188) Washington DC 20503.			
1. AGENCY USE ONLY *(Leave blank)*	**2. REPORT DATE** September 2005	**3. REPORT TYPE AND DATES COVERED** Master's Thesis	
4. TITLE AND SUBTITLE: Simulation of Wireless Propagation and Jamming In a High-Rise Building			**5. FUNDING NUMBERS**
6. AUTHOR(S) Yildirim Kaya			
7. PERFORMING ORGANIZATION NAME(S) AND ADDRESS(ES) Naval Postgraduate School Monterey, CA 93943-5000			**8. PERFORMING ORGANIZATION REPORT NUMBER**
9. SPONSORING /MONITORING AGENCY NAME(S) AND ADDRESS(ES) N/A			**10. SPONSORING/MONITORING AGENCY REPORT NUMBER**
11. SUPPLEMENTARY NOTES The views expressed in this thesis are those of the author and do not reflect the official policy or position of the Department of Defense or the U.S. Government.			
12a. DISTRIBUTION / AVAILABILITY STATEMENT Approved for public release; distribution is unlimited			**12b. DISTRIBUTION CODE** A

13. ABSTRACT (maximum 200 words)

Wireless Local Area Networks (WLANs) extend the usage of wired LANs from specific places within a building to the many mobile users whether in the building or outside. The wireless data is not only used by authorized users but also might be intercepted and altered by other unauthorized users. Therefore, the power of the transmitter is kept as low as possible to make it difficult for the others to intercept the signal. In the absence of interception, adversaries might attempt to jam the signal so that the network cannot operate properly. The purpose of present study is to investigate the effects of noise jamming against a WLAN in a high-rise building.

The building model was created by **Rhino**, a well known Windows-based computer drawing software. The jamming effects are simulated using **Urbana**. The LAN transmitter operates with an omni-directional antenna and 100 mW of power. The noise jammer has variable power levels of 10 W and 100 W. It uses a directional antenna. The signal-to jam-ratio (SJR) is computed for several floors in the building to determine if the jammer will disrupt the WLAN.

14. SUBJECT TERMS Urbana, Simulation of Wireless Propagation, Indoor Propagation, Antenna Fundamentals, Radio Wave Propagation, Wireless Networks, WLAN Security, Communication Jamming, Signal to Jam Ratio (SJR)			**15. NUMBER OF PAGES** 91
			16. PRICE CODE
17. SECURITY CLASSIFICATION OF REPORT Unclassified	**18. SECURITY CLASSIFICATION OF THIS PAGE** Unclassified	**19. SECURITY CLASSIFICATION OF ABSTRACT** Unclassified	**20. LIMITATION OF ABSTRACT** UL

NSN 7540-01-280-5500 Standard Form 298 (Rev. 2-89)
Prescribed by ANSI Std. 239-18

THIS PAGE INTENTIONALLY LEFT BLANK

SIMULATION OF WIRELESS PROPAGATION AND JAMMING IN A HIGH-RISE BUILDING

Yildirim Kaya
1st Lieutenant, Turkish Air Force
B.S., Turkish Air Force Academy, 1997

Submitted in partial fulfillment of the
requirements for the degree of

MASTER OF SCIENCE IN SYSTEMS ENGINEERING

from the

NAVAL POSTGRADUATE SCHOOL
September 2005

Author: Yildirim Kaya

Approved by: David C. Jenn
Thesis Advisor

Daniel C. Schleher
Second Reader

Dan C. Boger
Chairman, Department of Information Sciences

THIS PAGE INTENTIONALLY LEFT BLANK

ABSTRACT

Wireless Local Area Networks (WLANs) extend the usage of wired LANs from specific places within a building to the many mobile users whether in the building or outside. The wireless data is not only used by authorized users but also might be intercepted and altered by other unauthorized users. Therefore, the power of the transmitter is kept as low as possible to make it difficult for the others to intercept the signal. In the absence of interception, adversaries might attempt to jam the signal so that the network cannot operate properly. The purpose of present study is to investigate the effects of noise jamming against a WLAN in a high-rise building.

The building model was created by **Rhino**, a well known Windows-based computer drawing software. The jamming effects are simulated using **Urbana**. The LAN transmitter operates with an omni-directional antenna and 100 mW of power. The noise jammer has variable power levels of 10 W and 100 W. It uses a directional antenna. The signal-to jam-ratio (SJR) is computed for several floors in the building to determine if the jammer will disrupt the WLAN.

THIS PAGE INTENTIONALLY LEFT BLANK

TABLE OF CONTENTS

LIST OF FIGURES

LIST OF TABLES

THIS PAGE INTENTIONALLY LEFT BLANK

ACKNOWLEDGMENTS

I would like to express my sincere thanks to Professor David Jenn for his support, professional guidance and patience during this research. His knowledge in every aspect of this research led to the successful achievement and completion of this work possible. I would also like to thank Professor Daniel C. Schleher for agreeing to be the second reader. Their dedications to antenna theory and radar theory along with their proficiencies are sincerely appreciated.

Additionally, I would like to thank to my country Turkey and the Turkish Air Force for giving me the opportunity to undertake this study.

Finally, I would like to thank my wife Dilek for her endless love, support, patience, and understanding in completing my Master's Degree at the Naval Postgraduate School and this thesis. I dedicate this work to the love of my life Dilek.

THIS PAGE INTENTIONALLY LEFT BLANK

I. INTRODUCTION

A. WIRELESS NETWORKS

Wireless Local Area Networks (WLANs) have become more widespread since the ratification of the IEEE 802.11b standard. WLANs are widely deployed in places, such as office rooms, school campuses, companies, and even bookstores and coffeehouses [1]. Unlike the wired networks, 802.11-based WLANs broadcast radio frequency (RF) data and provide numerous benefits, such as

- ease of installation,
- cost effective,
- flexibility,
- mobility, and
- improved system reliability.

Some network managers have security fears regarding WLANs and prefer wired-LANs. With a WLAN, the data is broadcast between the client devices and the access points, which are also called WLAN endpoints. Any authorized or unauthorized WLAN client device, in range of the access point, can receive radio frequency data transmitted to or from the access point. Thus, the IEEE 802.11 specification, which applies to 802.11a, 802.11b and 802.11g, stipulates some security requirements as described in the next section.

B. WLAN VULNERABILITY AND SECURITY

Since radio waves travel through ceilings, floors, walls, windows and doors, unauthorized persons may receive the transmitted data by being on different floors or even outside the physical boundary of the building. If a WLAN does not have strict security measures, it is essentially giving wired-network access to everyone within range, including those outside of the building [2]. Since some companies deploy WLANs without all security features, WLANs attract the attention of hackers. A hacker, with a client device within radio frequency range of an access point, can intercept and disrupt the transmitted data if the data is not encrypted.

No one can guarantee a completely secure WLAN that will prevent unauthorized users from penetrating the network. This does not mean that security measures are

pointless. Ongoing security protections must be established and frequently updated. If the security protection is deployed and left static, an illegitimate user will likely get access to the network eventually.

Two main security approaches for WLANs are:

1. limit the signal coverage by using low power transmitters for a predefined physical zone cleared of illegitimate client devices, and
2. employ authentication and privacy features.

The first method can be achieved by either measurement or simulation using wireless toolsets. The properties of the antenna and the environment are defined in the software input file along with the placement of antennas. The power levels for coverage of an access point will be determined after running enough simulations. By antenna selection and placement, the signal coverage can be limited to the area occupied by legitimate users.

The second approach is to prevent unintended recipients from obtaining access to the WLAN when they are within the coverage of the network. Authentication, also called access control, prevents unauthorized clients from sending or receiving WLAN data. WLAN security for authentication includes the combination of

- Service Set Identifiers (SSIDs),
- Wired Equivalent Privacy (WEP) keys,
- Media Access Control (MAC) authentication, and
- open or shared key authentication.

WLAN privacy, on the other hand, ensures that only legitimate users can use the transmitted data. When the data is encrypted with a key that can be used only by legitimate recipients, the privacy of the WLAN is considered protected. Encrypting WLAN data shows that the integrity of the data remains uncorrupted during the transmission process [3].

In a military conflict, it might be necessary to "crash" or render inoperable an enemy's WLAN. If this is not possible by hacking into the network, then jamming is another alternative. The jammer transmits a strong noise or interference signal that prevents the WLAN receiver from detecting legitimate network signals.

To be effective, the jammer must transmit relatively high power or be very close to the WLAN access point. If the access point is in a physically secure area, then high jammer power or high antenna gain is required. If the jammer is located outside of the building, then the jammer propagation losses can be very high. On the other hand, if there are unprotected window openings, then the jammer signal can possibly penetrate into the building and effectively disrupt the network.

C. PREVIOUS STUDY

Indoor propagation was previously studied by Sumagaysay [4] and Boukraa [5]. The **Urbana** toolset was used predict the contours of WLAN power levels for a given building model. The WLAN signal distribution in single story and high-rise buildings at a frequency of 2.4 GHz was examined. Boukraa concluded that the signal levels for a 1-Watt transmitter could only be detected at the -70 dBm level within two floors of a high-rise structure. Two WLAN vulnerabilities were apparent. The first was the spread of the signal outside the building through the windows, and the second was the penetration of the signal through ceilings and floors.

D. OBJECTIVE AND APPROACH

A simple jamming transmitter can easily interfere with WLANs and make communications impossible. Other wireless services, such as Bluetooth, that operate in the same frequency range can also interfere with WLAN transmissions and reduce the usable bandwidth of the WLAN [3].

The purpose of this thesis is to examine the effects of noise jamming on a WLAN in a high-rise building. Specifically, the frequency of 2.4 GHz (IEEE 802.11b and IEEE 802.11g standard) was studied.

It was assumed that the security policies in the selected high-rise building were very stringent. The signal coverage was limited to the specific zone by using a low power transmitter of 100 mW [6], which was located in the most interior part of the building. It was also assumed that the policy did not allow electronic devices, which might possibly interfere with the WLAN. If the entire building is physically secure, then the closest point for jamming the WLAN would be about 30 meters away from the building, in a parking area. Chapter IV describes the properties of the jammer in detail.

E. THESIS OUTLINE

Following the Introduction, Chapter II discusses radiowave propagation and interference as it relates to wireless propagation. Chapter III gives an overview of the **Rhino** software which is used to create the building model, and the **Urbana** software, which is used to perform the propagation simulations. Chapter IV describes the properties of the jammer. Simulation and analysis of wireless propagation, interference, and jamming in a high-rise building is also contained in this chapter. Chapter V summarizes the results of the simulations and gives recommendations for future work.

II. RADIO WAVE PROPAGATION

Electromagnetic waves propagate by a variety of mechanisms that are generally categorized as reflection, diffraction, and scattering. In an indoor environment, where there is no direct line-of-sight (LOS) between the transmitter and the receiver, diffraction and multiple reflections from different objects, cause the electromagnetic waves to propagate along different paths and have different arrival times and phase shifts. Multipath fading happens because of the interaction between these waves. [7]

A. PROPAGATION MECHANISMS

1. Electromagnetic Fields and Waves

Electromagnetic waves consist of sinusoidal electric and magnetic fields, which are completely described by Maxwell's equations:

$$\nabla \times \vec{E} = -\mu \frac{\partial \vec{H}}{\partial t} \tag{2.1}$$

$$\nabla \times \vec{H} = \vec{J} + \varepsilon \frac{\partial \vec{E}}{\partial t} \tag{2.2}$$

$$\nabla \cdot \vec{H} = 0 \tag{2.3}$$

$$\nabla \cdot \vec{E} = \rho_v / \varepsilon \tag{2.4}$$

where $\vec{E}$ (V/m) is the electric field intensity, $\vec{H}$ (A/m) is the magnetic field intensity, $\vec{J}$ (A/m^2) is the volume current density, and ρ_v (C/m^3) is the volume charge density. Electrical properties of a medium through which the waves are propagating are specified by its constitutive parameters, such as permittivity (ε in F/m), permeability (μ in H/m), and conductivity (σ in S/m).

Assuming a $e^{j\omega t}$ time dependence, the complex permittivity and permeability are

$$\varepsilon = \varepsilon' - j\varepsilon'' \tag{2.5}$$

$$\mu = \mu' - j\mu'' . \tag{2.6}$$

If the medium is lossy, then the imaginary terms are nonzero.

The relative values for ε and μ are

$$\varepsilon = \varepsilon_0 \varepsilon_r \tag{2.7}$$

$$\mu = \mu_0 \mu_r \tag{2.8}$$

where ε_r is the relative permittivity, and μ_r is the relative permeability. Both can be complex in accordance with Equations (2.5) and (2.6). In free space, which is a lossless medium

$$\varepsilon = \varepsilon_0 \tag{2.9}$$

where $\varepsilon_0 = 8.8542 \times 10^{-12}$ F/m, and

$$\mu = \mu_0 \tag{2.10}$$

where $\mu_0 = 4\pi \times 10^{-7}$ H/m. The majority of the materials in an indoor environment are nonmagnetic. Thus, $\mu = \mu_0$ is assumed for further calculations.

In terms of the conductivity of the medium, the complex relative dielectric constant of the material is [8]

$$\varepsilon_r = \varepsilon_r' - j\frac{\sigma}{\omega \varepsilon_0} \tag{2.11}$$

where σ is the conductivity of the material (S/m), $\omega = 2\pi f$ is the radian frequency (rad/sec), and f is the frequency (Hz). Finally, the intrinsic impedance of the medium is

$$\eta = \sqrt{\frac{\mu}{\varepsilon}}. \tag{2.12}$$

The wave equations can be derived for the electric and magnetic fields. They solve Maxwell's equations for a source free region

$$\nabla^2 \vec{E} - \gamma^2 \vec{E} = 0 \tag{2.13}$$

$$\nabla^2 \vec{H} - \gamma^2 \vec{H} = 0. \tag{2.14}$$

Plane waves are the simplest solutions to the wave equations. A plane wave propagating in the z direction is given by the phasor expression

$$\vec{E}(z) = \hat{x}E_0 e^{-\gamma z} \tag{2.15}$$

where E_0 is the electric field at the source, and γ is the propagation constant, which is

$$\gamma = j\omega\sqrt{\mu\varepsilon} = \alpha + j\beta \tag{2.16}$$

where α is the attenuation constant (Np/m), $\beta = \frac{2\pi}{\lambda}$ is the phase constant (rad/m), and λ is the wavelength. The phase velocity of electromagnetic wave in a medium depends on the permittivity and permeability of the medium

$$u_p = \frac{\omega}{\beta}\ . \tag{2.17}$$

In free space, $u_p = c = \frac{1}{\sqrt{\mu_0 \varepsilon_0}} = 2.998 \times 10^8 \text{ m/s}$.

2. Reflection and Refraction

When an electromagnetic wave propagates in one medium and impinges upon another medium with different electrical properties, reflection occurs. When the boundary has large dimensions relative to the wavelength of the propagating wave, then high frequency approximation (i.e., ray tracing) applies.

The wave will also be partially refracted into the second medium unless it is a perfect conductor. If the second medium is a perfect electric or magnetic conductor, there will be no refraction, and the entire incident wave is reflected back into the first medium. The reflected and refracted wave intensities are also related to the properties of the incident wave, such as the wave polarization, angle of incidence, and the frequency of the propagating wave. [7] A sample ray diagram of a plane wave incident on an interface between two dielectrics is illustrated in Figure 1.

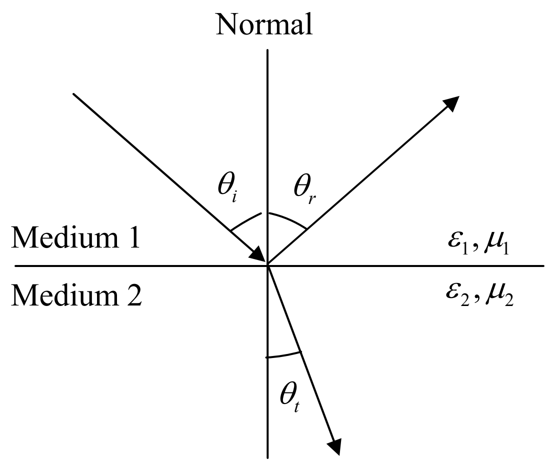

Figure 1. A sample of reflected and refracted waves

The angle of the reflected wave is equal to the angle of incidence by Snell's law of reflection

$$\theta_i = \theta_r \ . \tag{2.18}$$

This is referred to as specular reflection. The index of refraction of a medium is the ratio of the phase velocity in free space to the phase velocity in the medium. By Snell's law of refraction

$$n_1 \sin\theta_i = n_2 \sin\theta_t \tag{2.19}$$

where n_1 and n_2 are the indices of refraction of media 1 and 2, respectively. The index of refraction is related to the dielectric constant, $n = \sqrt{\varepsilon_r}$. When $n_1 < n_2$, it follows that $\sin\theta_i > \sin\theta_t$ and also that $\theta_i > \theta_t$. Thus, it can be said that the ray entering a higher index medium bends toward the normal as in Figure 2.(a). The reverse is also true, that is, the ray entering a lower index medium bends away from the normal as in Figure 2.(b) [9].

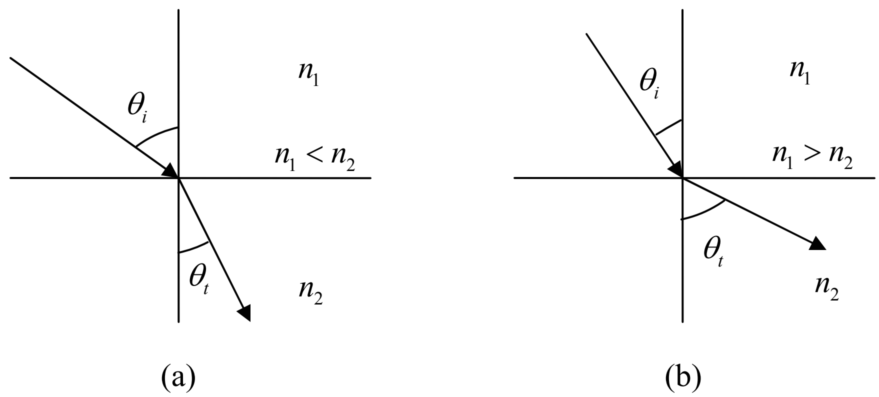

Figure 2. Bending of rays at an interface, (a) the ray entering a higher-index medium, (b) the ray entering a lower index-medium

3. Diffraction

Diffraction occurs when there is a surface that has a discontinuity between the transmitter (Tx) and the receiver (Rx), and obstructs the direct path of the electromagnetic wave. The secondary wavelets created at the edge propagate behind the obstacle into the shadow. Thus, there can be sufficient field strength for reception in the shadowed region.

The intensity of diffraction depends on the geometry of the obstacle, and amplitude and polarization of the incident electromagnetic wave. A sample of edge diffraction is illustrated in Figure 3.

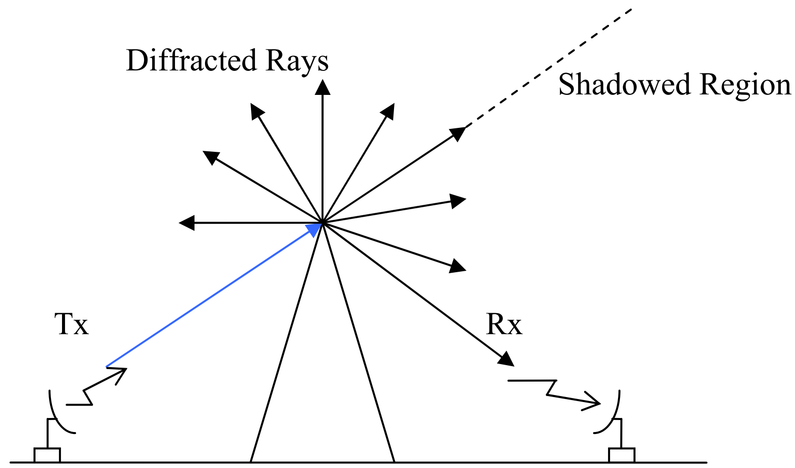

Figure 3. Geometry of wedge diffraction

4. Scattering

When electromagnetic waves arrive at the receiver, the received signal is often stronger than what is expected based on specular reflection and diffraction. Scattering occurs when a electromagnetic wave impinges upon a rough surface or object which has small dimensions relative to the wavelength. This is because scattered waves propagate in many directions due to isotropic scattering. In an indoor environment, such as in offices, a variety of small objects (e.g., cups, computer mouse, staplers, etc.) scatter waves in all directions. [7]

B. ANTENNA FUNDAMENTALS

An antenna may be defined as a transducer that provides a means for radiating or receiving electromagnetic waves. Antennas are made in different sizes and shapes, and are used in various areas, such as [10]

- radiowave communication systems (e.g., WLANs),
- cellular systems,
- radio and television broadcasting and reception, and
- radar systems.

An isotropic antenna is a hypothetical antenna that has a uniform radiation pattern in all directions. It is used as a reference for defining the directive properties of all antennas.

1. Antenna Radiation Pattern

The antenna radiation pattern is the angular variation of radiation fields at a fixed distance from the transmitting antenna [11]. The antenna pattern is represented by $F(\theta,\phi)$ for the field and $P(\theta,\phi)$ for the power. The general normalized power pattern in decibels is

$$P(\theta,\phi) = 20\log\left|\frac{F(\theta,\phi)}{F_{\mathrm{max}}}\right| \ \ [\mathrm{dB}] \tag{2.20}$$

where F_{max} is the main lobe magnitude.

The antenna pattern, as shown in Figure 4, has main, side and back lobes. Side and back lobes together are also called *minor lobes*. The side lobe level (SLL) is the ratio of the side lobe peak to the main lobe peak

$$\mathrm{SLL} = 20\log\left|\frac{F_{\mathrm{SLL}}}{F_{\mathrm{max}}}\right| \ \ [\mathrm{dB}] \tag{2.21}$$

where F_{SLL} is the highest side lobe magnitude. The angular width of the main lobe is the angle between first nulls and is generally represented by half-power beam width (HP or HPBW). The HPBW is also known as the 3-dB beam width,

$$\mathrm{HPBW} = \left|\theta_{\mathrm{HP_{left}}} - \theta_{\mathrm{HP_{right}}}\right| . \tag{2.22}$$

A sample of an antenna radiation pattern is illustrated in Figure 4.

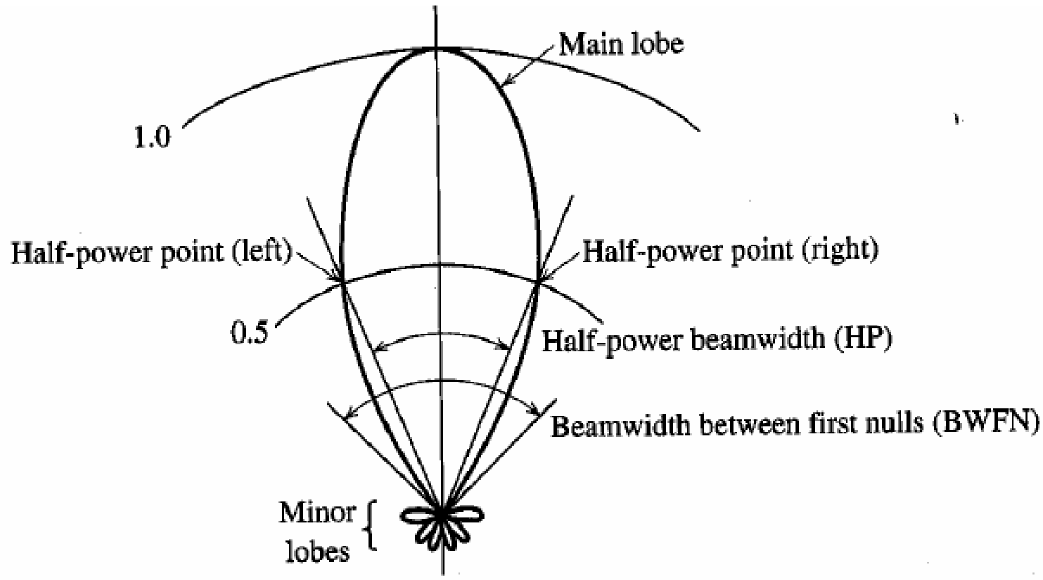

Figure 4. Sample polar plot of antenna radiation pattern (From Ref. [11].)

2. Antenna Directivity

The directivity is the ratio of maximum normalized power density in the main beam direction of the radiation pattern to the average power density of the antenna

$$D = \frac{S}{S_i} \tag{2.23}$$

where S $(\mathrm{W/m^2})$ is the maximum power density, and S_i is the average power density. It is assumed that all of the power in an antenna is radiated. When describing the pattern properties of an antenna, the radiation pattern is compared to spatial distribution of an isotropic antenna. For an isotropic antenna, the directivity is equal to one. A sample of an antenna radiation pattern and its directivity is illustrated in Figure 5.

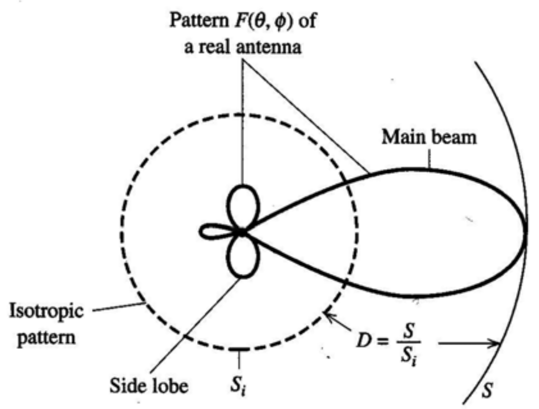

Figure 5. Illustration of radiation pattern and directivity (From Ref. [11].)

3. Antenna Gain

The directivity is reduced due to losses in the antenna. This loss defines the efficiency of the antenna, e. The gain is then the product of the directivity and the efficiency. If the efficiency of the antenna is 100%, the gain is equal to directivity. In practice, the gain of a lossless antenna is

$$G = \frac{4\pi A_e}{\lambda^2} \qquad (\text{for } A_e >> \lambda^2) \tag{2.24}$$

where A_e is the effective area of the antenna. The gain of an antenna is also approximately equal to [12]

$$G \approx \frac{26{,}000}{\theta_B \phi_B} e \tag{2.25}$$

where θ_B and ϕ_B are the elevation and azimuth HPBWs, respectively, in degrees.

4. Antenna Polarization

The antenna polarization refers to the vector direction of the wave radiated by the transmitting antenna in terms of the time-varying orientation of the electric field. The tip of the electric field vector traces a path in space, and generally, it is elliptical [10]. This is called *elliptical polarization.* If the path is a circle or a straight line, then the polarization is called *circular* or *linear polarization*, respectively.

In most wireless applications, the transmitting and the receiving antennas are linearly polarized. Polarization mismatch loss occurs if the transmitting and receiving antennas are not similarly polarized.

C. FREE-SPACE LINK EQUATION

Assuming no polarization mismatch loss and no obstruction between the transmitting and the receiving antennas, as shown in Figure 6, the received signal power in free-space can be expressed by Friis's transmission formula [11]

$$P_r = \frac{P_t G_t G_r \lambda^2}{\left(4\pi d\right)^2} \tag{2.26}$$

where P_t is the transmitted power in watts, d is the distance between the transmitting and the receiving antennas, and G_t and G_r are the gains of transmitting and the receiving antennas, respectively.

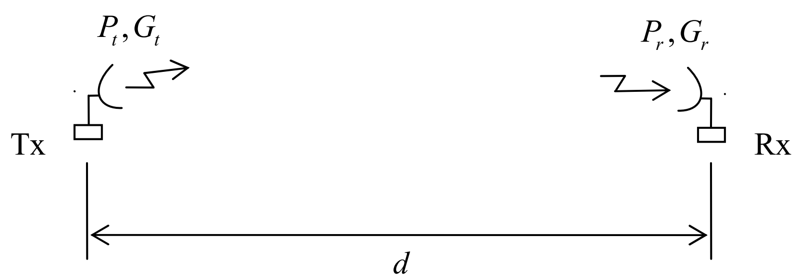

Figure 6. A free-space communication link

The *effective isotropically radiated power* (EIRP) is the transmitted power into the antenna multiplied by the power gain of the transmitting antenna in a given direction relative to an isotropic antenna

$$\text{EIRP} = P_t G_t \ . \tag{2.27}$$

It is also called the *effective radiated power* (ERP). Usually, the free-space link equation is written in decibels

$$P_r = P_t + G_t + G_r - \left(L_{fs} + L\right) \ \ \text{[dB]} \tag{2.28}$$

where L_{fs} and L are the free-space path loss and the other losses, respectively. The free-space path loss is proportional to the inverse square of the distance between transmitting and receiving antennas and is frequency dependent

$$L_{fs} = 10\log\left(\frac{4\pi d^2}{\lambda^2}\right) \text{ [dB]} . \tag{2.29}$$

D. INDOOR PROPAGATION

Indoor propagation is affected by reflection, diffraction, and scattering as it is for outdoor propagation. However, characterizing indoor propagation differs from outdoor propagation modeling since the distances are much smaller and the environmental variability is much greater. The building type, construction materials, and indoor layout (open or closed doors) contribute to the received signal level and indoor path loss [7].

1. Log-Distance Path Loss Model

For both outdoor and indoor propagation, the average received signal power decreases logarithmically with distance [7]

$$\overline{PL} = \overline{PL}(d_0) + 10n\log\left(\frac{d}{d_0}\right) \text{ [dB]} \tag{2.30}$$

where PL is the path loss, d_0 is the reference distance, d is the distance between the transmitter and the receiver, and n is the path loss exponent which depends on the specific propagation environment. The exponent n will have a larger value when obstructions are present between the transmitter and the receiver. The bars in Equation (2.30) denote the average path loss values for a given value of d. Table 1 shows the path loss exponents (n) for different environments.

Environment	Path Loss Exponent
Free space	2
Urban area cellular radio	2.7 to 3.5
Shadowed urban cellular radio	3 to 5
In building line-of-sight (LOS)	1.6 to 1.8
Obstructed in building	4 to 6
Obstructed in factories	2 to 3

Table 1. Path loss exponents, n, for different environments (From Ref. [7].)

2. Attenuation Model

The building type and obstacles in the building degrade the performance of wireless systems indoors [7]. A common attenuation factor model is

$$\overline{PL}(d) = \overline{PL}(d_0) + 20\log\left(\frac{d}{d_0}\right) + \alpha d + FAF + \sum PAF \quad [\text{dB}] \tag{2.31}$$

where α is the attenuation constant in dB/m, FAF is the floor attenuation factor, PAF is the partition attenuation factor for an obstruction which blocks the LOS between the transmitter and the receiver. As shown in Equation (2.31), in multi-floor buildings, the path loss depends on the free-space loss plus an additional loss, which increases exponentially with distance.

3. Ray Tracing Model

New methods for predicting signal coverage in indoor environments involve some computational electromagnetic tools, such as **Urbana**, which is described in detail in the next chapter. This software uses a three-dimensional (3-D) ray-tracing engine, which also includes

- antenna pattern and polarization effects,
- fading and co-channel interference, and
- multipath and diffraction effects.

With the help of these computer-aided design tools, predictions and measurements of the signal coverage may be simultaneously viewed, manipulated and optimized [7].

E. INTERFERENCE AND COMMUNICATION JAMMING

Interference occurs when two signals at the same frequency arrive at a single receiver. As shown in Figure 7, one of these signals is considered the desired signal and the other is an interfering signal. The interfering signal could be either intentional or unintentional. If it is intentional, then the objective of the interfering signal is to reduce the quality of the desired signal to an unusable level [13].

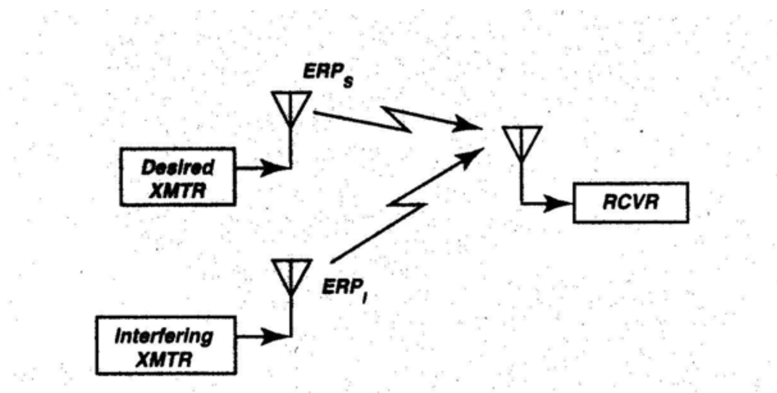

Figure 7. Sample link from each transmitter to the receiver (From Ref. [13].)

The power difference between the desired signal and the interfering signal, assuming that the receiving antenna has the same gain to both signals, is written in decibels

$$P_S - P_I = ERP_S - ERP_I + 20\log(d_I) - 20\log(d_S) \text{ [dB]} \tag{2.32}$$

where

- P_S is the received power from the desired source,
- P_I is the power from the interfering source,
- ERP_S is the effective radiated power of the desired signal,
- ERP_I is the effective radiated power of the interfering signal,
- d_S is the path distance to the desired antenna, and
- d_I is the distance to the interfering antenna.

The same link equation can be applied to the jammer as for the desired transmitter. The ratio of received power gives the *signal-to-jam ratio* $\left(S/J\right)$, which is then [14]

$$S/J = ERP_S - ERP_J + G_R - G_{RJ} + 20\log(d_J) - 20\log(d_S) \text{ [dB]} \tag{2.33}$$

where G_R and G_{RJ} are the gains of the receiving antenna toward the desired transmitter and toward the jammer, respectively. If the gain of the receiving antenna is omni-directional in azimuth, G_R and G_{RJ} cancel each other. Otherwise, if the receiving antenna

has a narrow beam and is pointed at the desired transmitter, then the jammer has to transmit enough power to overcome the difference in the antenna gain.

In this thesis, the objective is to inject an interference signal, as in noise jamming, into the receiver such that the actual signal is submerged in the interference [15]. This type of jamming is also known as denial jamming.

This chapter is mainly concerned radiowave propagation mechanisms, antenna fundamentals, the free-space link equation, and interference and communication jamming. The next chapter discusses the software tools, which are used for the model and the simulations.

III. SOFTWARE DESCRIPTIONS

A. INTRODUCTION

Urbana is a Unix-based program developed by Science Application International Corporation (SAIC). The main components of **Urbana** are **Cifer**, **XCell**, and **Urbana** [16].

Urbana, being a powerful Computational Electromagnetic (CEM) tool, determines the signal level for wireless networks with predefined inputs, such as, building geometry, antenna types, frequency, and polarization. There is capability to analyze [17]

- urban propagation,
- indoor and outdoor propagation,
- collision avoidance radar, and
- antenna studies.

The purpose of this research is to analyze the effects of noise jamming on wireless systems operating inside a high-rise building.

B. SOFTWARE TOOLS

1. Rhino

Rhino Version 2.0 software, which runs on Windows platforms, was chosen to generate the high-rise building. It is a very powerful, and user friendly CAD software. **Rhino** is a very effective toolset to create, analyze, render, edit, and build a 3-D model precisely. [18] The individual components of the model for this project were created separately by **Rhino**, such as, the outer walls, the inner walls, the doors, the windows, and the elevators. This allowed the materials for each group to be changed independent of the others.

Rhino supports many file formats. For this project, the *.*iges* format was chosen. This format was readable by **Cifer**, as described in the next section. A sample of the four-view **Rhino** editor is illustrated in Figure 8.

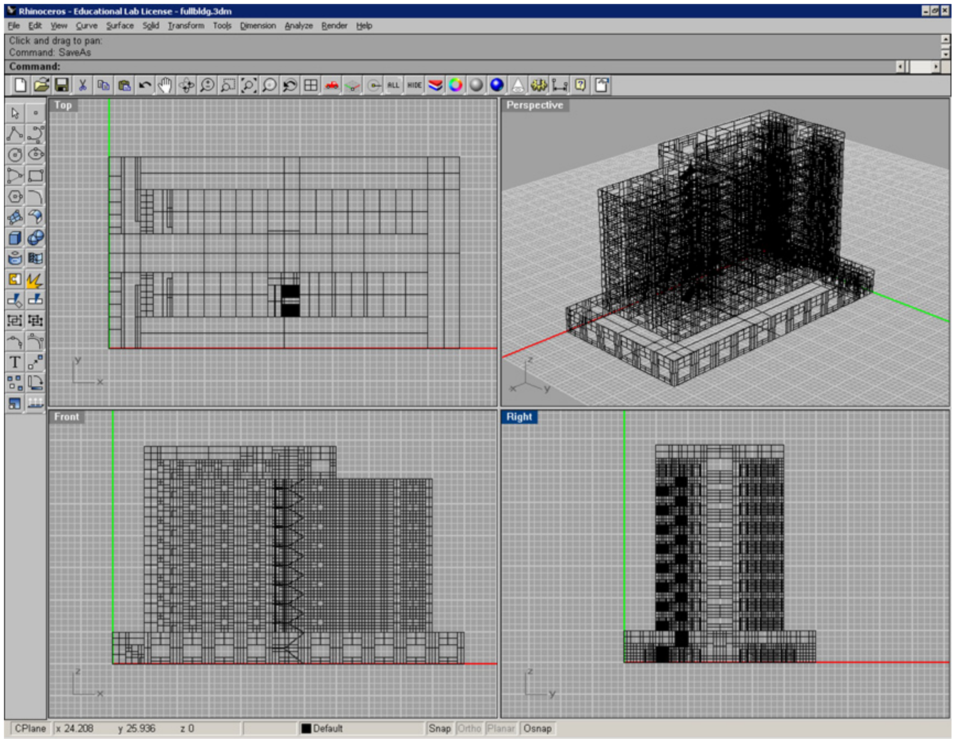

Figure 8. A sample Rhino GUI editor

2. Cifer

Cifer is primarily used to convert files imported from CAD software programs into the facet file format required by **Urbana**. All the predefined *.*iges* files for the individual building components imported from **Rhino** were converted to *.*facet* files with different ICOAT numbers. Thus, each ICOAT number corresponds to a unique material. Zero is the ICOAT value for a perfect electric conductor (PEC).

The model is completed by combining all of the individual *facet* files into one. For instance, the combination of the outer walls and the inner walls is subsequently combined with the doors and so forth, to obtain a single file for the entire building.

Cifer is also capable of extracting edges from a *facet* file. The *consolidate* mode is also used to consolidate facets and edges. A sample graphical user interface (GUI) is illustrated in Figure 9.

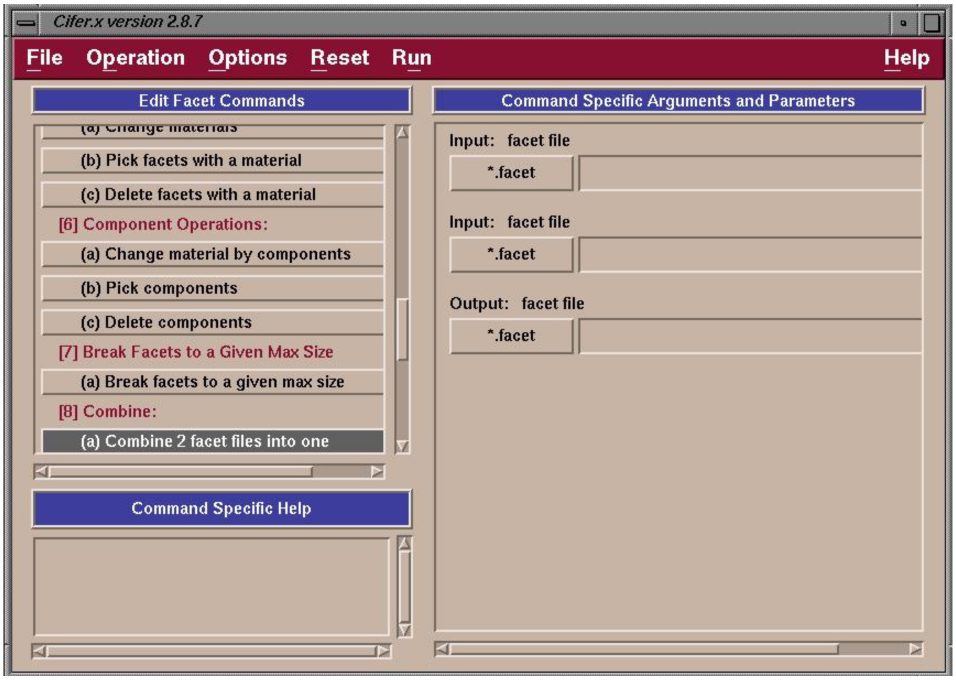

Figure 9. A sample Cifer GUI editor

3. XCell

XCell is used to view and modify the *facet* files created by **Cifer** and to view the signal contours generated by the programs *f2f* or *f2fd*. One can view the 3-D perspective of signal strengths in and around the building model in color-coded plots. It is also possible to view *facet* files together with *antenna* files and *edge* files at the same time. A sample GUI for **XCell** is illustrated in Figure 10.

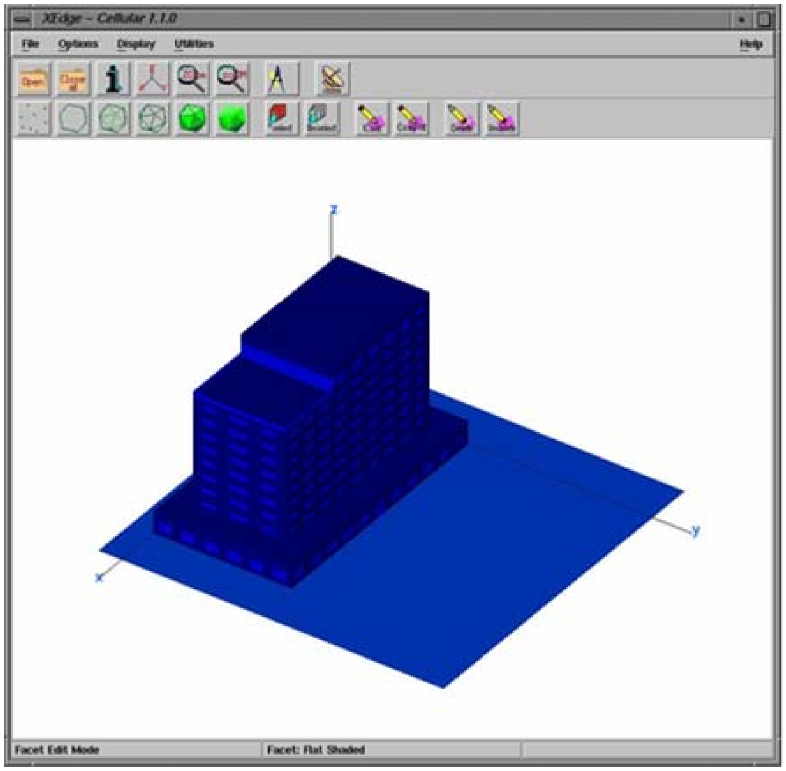

Figure 10. A sample XCell GUI editor

4. Urbana

Urbana uses a 3-D ray tracing engine to characterize electromagnetic wave propagation. The ray tracing engine has a high-speed algorithm to implement Geometric Optics (GO), Physical Optics (PO) and the Geometrical Theory of Diffraction (GTD). A sample **Urbana** file appears in the Appendix. The key inputs to the **Urbana** code (*.*ur_input*) are

- facet model for the CAD geometry file (*.*facet*),
- frequency,
- antenna file, which includes antenna pattern, power, and polarization (*.*antenna*),
- observation point file (*.*txt*),
- edge file for edge diffraction (*.*edge*), and
- building material properties, such as, concrete, ground, wood, glass, and dielectrics.

The key output to the **Urbana** code is a composite field file (*.*field*) for the observation plane, which is defined in the input file.

a. *Generating Input Data Files (Step 1)*

The building model is represented by surfaces of triangular facets. As described in Section 2, **Rhino** is used to generate the high-rise building model in **.iges* format. **Cifer** is then used to convert the output file to the DEMACO facet file format. Each facet file is characterized by the coating material defined by the input variable ICOAT. Cifer is also used to extract edges (**.edge*) from the facet file. **Urbana** also requires a set of observation points at which the field is to be computed. To build an observation point list, a **Matlab** script file is run and the output file is saved in ASCII **.txt* format. Step 1 is illustrated in Figure 11.

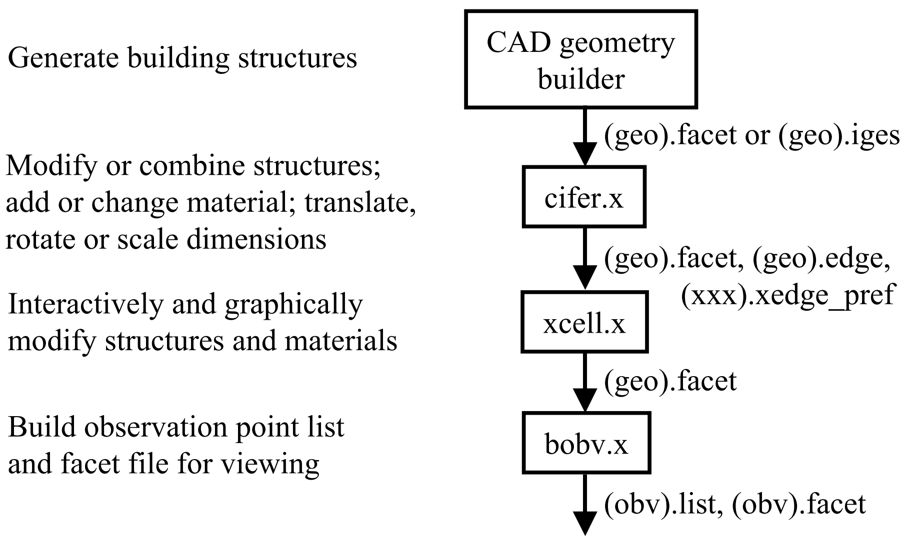

Figure 11. Generating input data file for **Urbana** (From Ref. [19].)

b. *Generate Urbana Input File and Run Urbana (Step 2)*

The **Urbana** input file (**.ur_input*) is composed of the key input parameters and the file names described above. After executing **Urbana**, the output is summarized in the composite field file (**.field*). This step is illustrated in Figure 12.

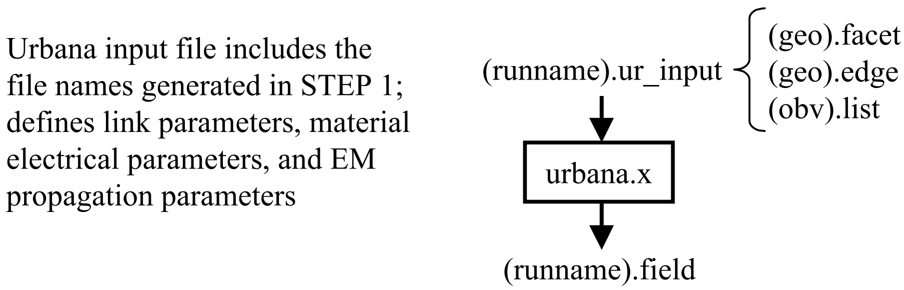

Figure 12. Process for running **Urbana** (From Ref. [19].)

c. *Post Processing (Step 3)*

After getting the **.field* file, the command *f2f* is used to convert it to a **.facet* file for viewing the signal back in **XCell**. There are some selections with this command, such as, magnitude of electric field level, antenna power level, color bar settings, clip minimum-maximum, and range minimum-maximum. **XCell** is used to view the **.facet* file. This step is illustrated in Figure 13.

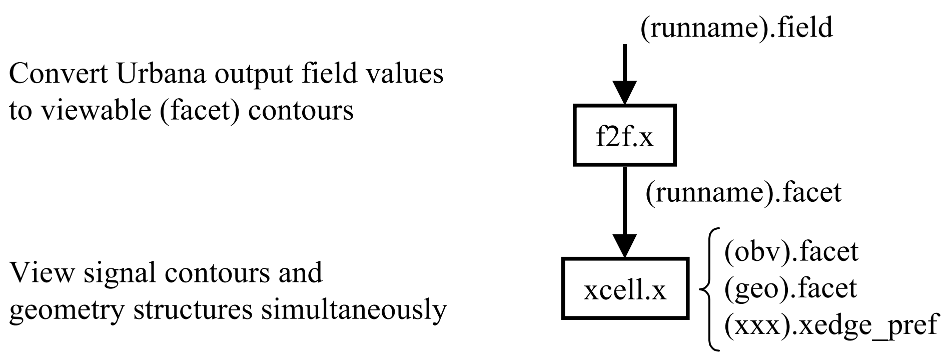

Figure 13. **Urbana** post-processing (From Ref. [19].)

C. DESIGNING MODEL

As discussed in Section B, the model is built using the Rhino software. The building is a ten-story office or hotel building. The first floor has a larger area than the other floors. The dimensions of first floor are illustrated in Figure 14.

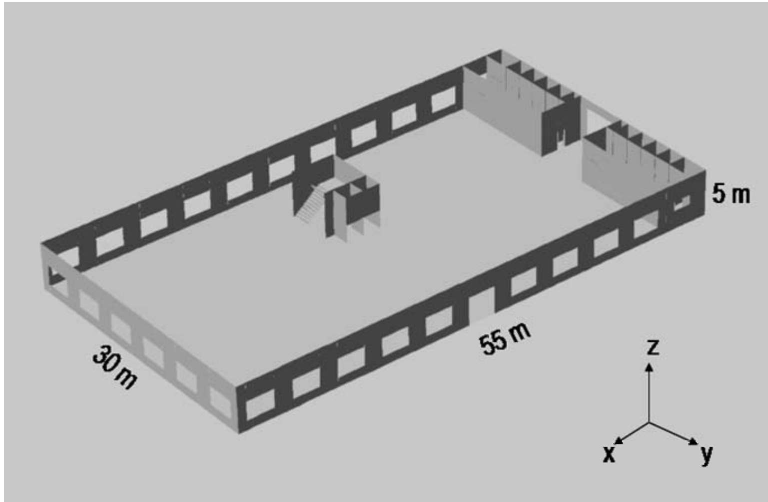

Figure 14. First floor lobby area

Floors 2 through 9 are identical. They consist of two rows of rooms (or offices) with elevators and stairwell. Also, restrooms are located at one end of the building, as shown in Figure 15.

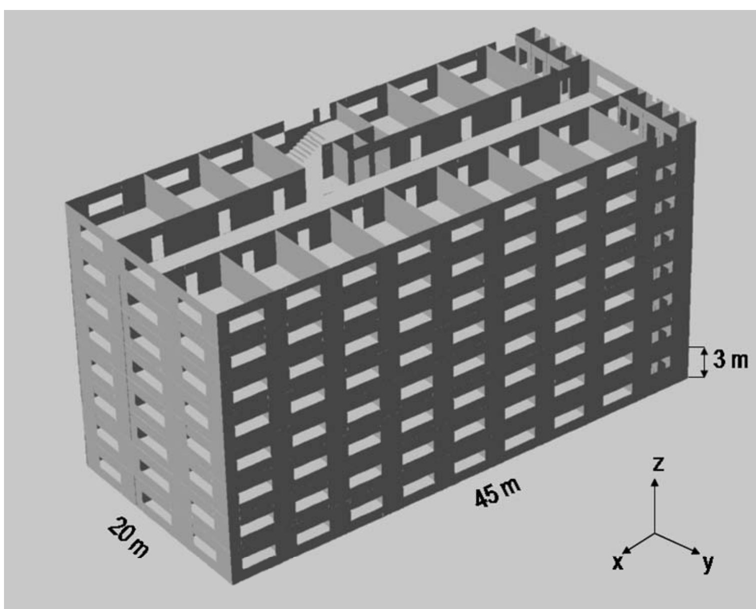

Figure 15. Floors two through nine (office areas or hotel rooms)

The roof has an open patio area and an enclosed restaurant area. The dimensions of the roof are illustrated in Figure 16.

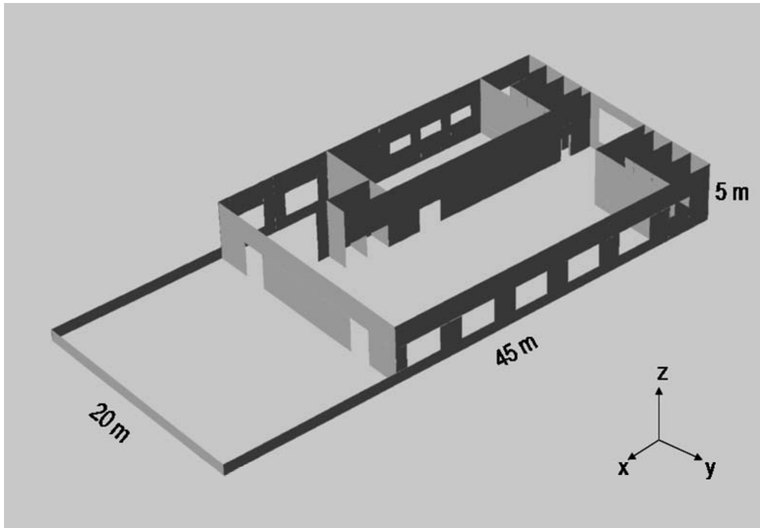

Figure 16. Tenth floor with patio and restaurant

Finally, a flat ground plane is located under the building to simulate the ground with the dimensions as shown in Figure 17.

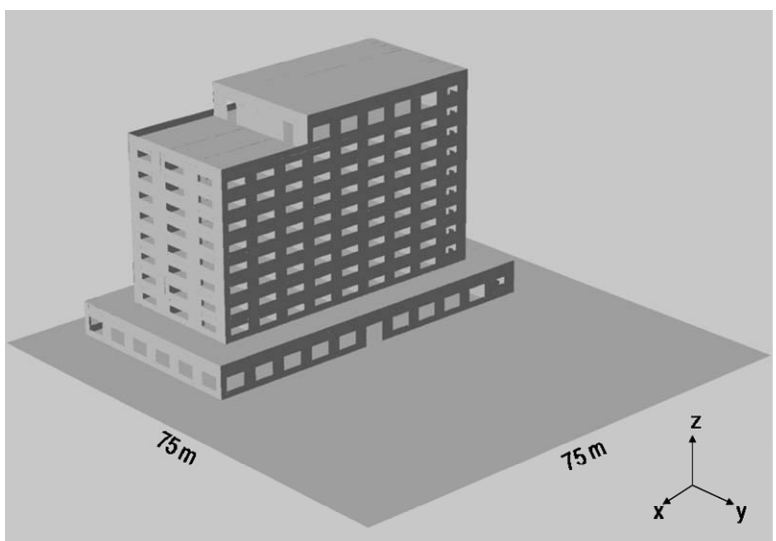

Figure 17. The whole building model with the ground

The model is composed of six different materials, and each one is given a different ICOAT value after it is imported into **Cifer**. All parts are then combined by

using the "combine two *facet* files" command in **Cifer**. The building consists of the following materials:

- The outer walls (ICOAT=1) which are concrete and 0.3 m thick.
- The inner walls (ICOAT=2) also concrete but 0.1 m thick.
- The doors (ICOAT=3) which are wood and 0.05 m thick.
- The windows (ICOAT=4) are glass and 0.025 m thick.
- The elevator doors (ICOAT=0) are PEC and 0.05 m thick.
- The ground (ICOAT=6) is considered as a 0.1 m thick concrete layer over a semi-infinite conductor.

Each component has its own permeability, permittivity, resistivity, and thickness values specified in the *.*ur_input* file as shown in Table 2.

COATING MATERIAL	**Material**	**ICOAT**	**Permeability** (μ', μ'')	**Permittivity** $(\varepsilon', \varepsilon'')$	**Resistivity** (ohm)	**Thickness** (meters)
Outer Walls	Concrete	1	1, 0	10.1, -0.5	1e30	0.3
Inner Walls	Concrete	2	1, 0	10.1, -0.5	1e30	0.1
Doors	Wood	3	1, 0	3, -0.67	1e30	0.05
Windows	Glass	4	1, 0	6, 0	1e30	0.025
Elevator Doors	Metal	0(PEC)	1, 0	1, 0	0	0.05
Ground	Concrete	6	1, 0	3, 0	1e30	0.1

Table 2. Properties of each coating material

This chapter dealt mainly with explaining different software tools used to perform the simulations. The next chapter concerns creating the jammer antenna and seeing the effects of noise jamming on the model.

THIS PAGE INTENTIONALLY LEFT BLANK

IV. URBANA SIMULATIONS, ANALYSIS AND RESULTS

The previous chapter described the software used to develop the high-rise building model and a brief introduction to propagation modeling. This chapter describes the WLAN and the jammer system and antenna properties as well as the placements, the simulations and their results. Indoor propagation and signal-to-jam ratio (SJR) are also evaluated.

The first step is to study the indoor propagation and signal distribution for the entire building model without the jammer. Next, the effects of the jammer, which could possibly have different HPBWs and power levels, are calculated inside the building model. Finally, the presence of the jammer on the WLAN system is studied. By examining the SJR, the jamming contours are generated for the WLAN network.

A. WLAN TRANSMITTER ANTENNA

Currently, most WLAN devices operate with vertically polarized antennas. A vertically polarized antenna generally has a slightly higher signal level than a horizontally polarized antenna in an indoor environment [20]. In the simulations, the transmitter antenna is considered as an access point and is located in the most interior part of the building model, i.e., in the middle of the fifth floor. Also, to provide network coverage where needed, an omni-directional WLAN antenna is used. A transmitter with a power of 100 mW with 802.11b/g standard has a data rate from 11 Mbps to 54 Mbps. The maximum range of a typical access point configured with a 2.2 dBi dipole antenna for 802.11b/g is shown in Table 3 [21]. Thus, 2.4 GHz, an omni-directional half-wave dipole antenna, transmitting a power of 100 mW is chosen for the simulations. Figure 18 shows the 3-D radiation pattern of a dipole antenna.

Typical Indoor Data Rate	Range
54 Mbps	27 m (90 ft)
18 Mbps	54 m (180 ft)
11 Mbps	48 m (150 ft)
6 Mbps	91 m (300 ft)
1 Mbps	124 m (410 ft)

Table 3. The maximum range and the data rate of a typical access point (From Ref. [21].)

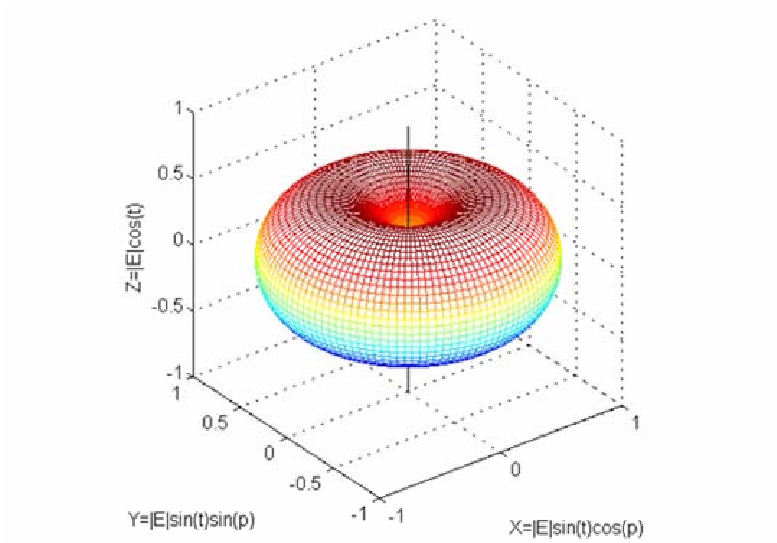

Figure 18. Normalized radiation pattern of a dipole antenna (From Ref. [19].)

B. JAMMER ANTENNA

Since the entire building is physically secure against possible inside jammers as mentioned in Chapter I, the jammer is considered to be located about 30 meters away from the building, in the parking area. The effects of three different jammers each with two different power levels are studied against the building model. Jammer 1, jammer 2 and jammer 3 have 10°-HPBW, 20°-HPBW, and 30°-HPBW, respectively. Each jammer antenna transmits 10 W and 100 W.

It is also considered to use a vertically polarized directional antenna for the jammer to obtain maximum jamming effectiveness against the WLAN in the building. A **Matlab** code that plots the pattern of the jamming antenna was developed. The antenna radiation pattern of the jammer is zero in the rear hemisphere of the jammer antenna. The

user simply inputs the HPBW, and the generated ASCII pattern file is exported to **Urbana** in **.dat* file format. The **Matlab** code appears in the Appendix.

Jammer 1 antenna has a 0.3650 meter radius and 25.2713 dBi of directivity. Sample **XCell** views of the 10°-HPBW jammer antenna pattern, with 10 W and 100 W, are illustrated in Figure 19.

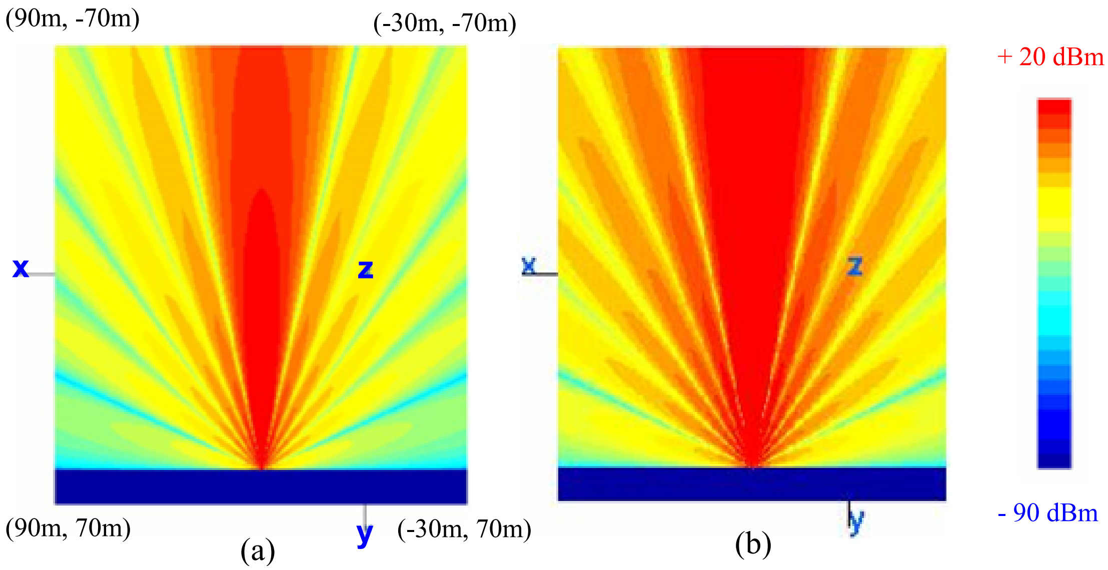

Figure 19. The radiation pattern of 10°-HPBW jamming antenna with (a) 10 W, (b) 100 W

Jammer 2 antenna has a 0.1825 meter radius and 19.2507 dBi of directivity. Sample **XCell** views of the 20°-HPBW jammer antenna pattern, with 10 W and 100 W, are illustrated in Figure 20.

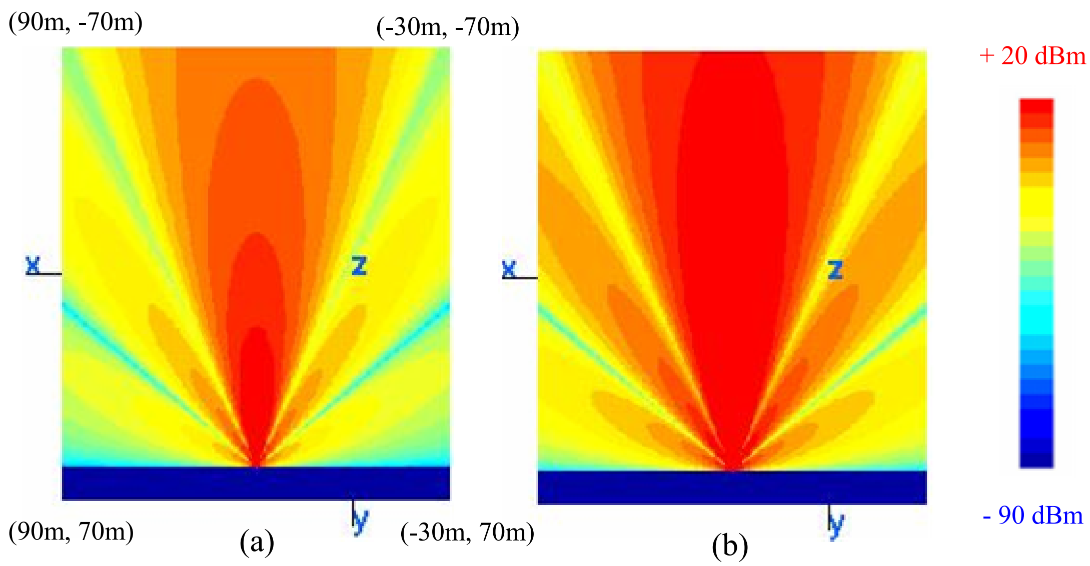

Figure 20. The radiation pattern of 20° -HPBW jamming antenna with (a) 10 W, (b) 100 W

Jammer 3 antenna has a 0.1217 meter radius and 15.7288 dBi of directivity. Sample **XCell** views of the 30° -HPBW jammer antenna pattern, with 10 W and 100 W, are illustrated in Figure 21.

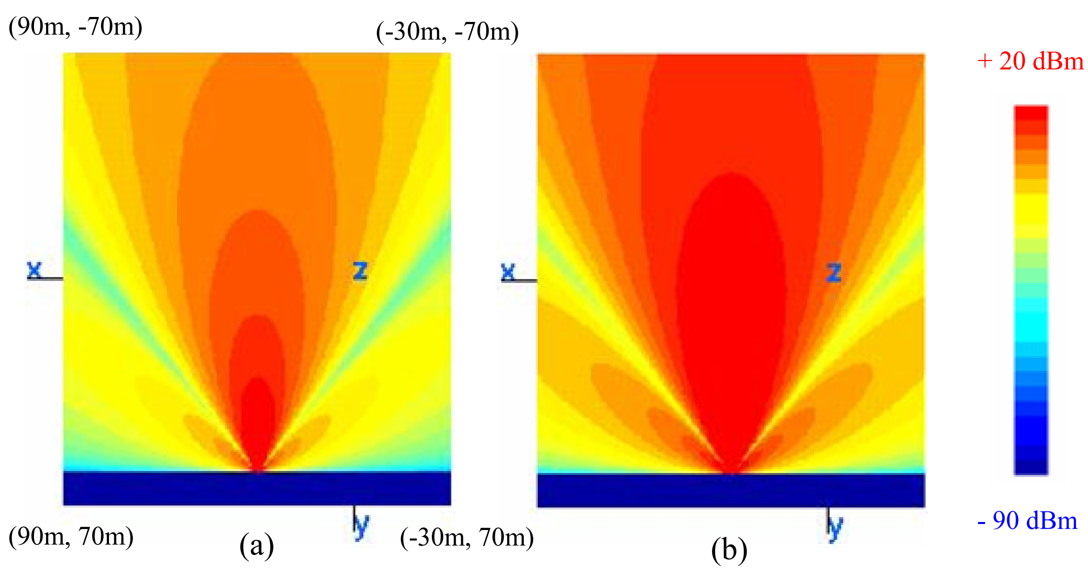

Figure 21. The radiation pattern of 30° -HPBW jamming antenna with (a) 10 W, (b) 100 W

For the simulations, each jammer antenna is then tilted 30° with respect to the ground to aim the main beam approximately at the middle of the building. Figure 22 shows the 10°-HPBW jammer antenna pattern when tilted up to the center of the building model.

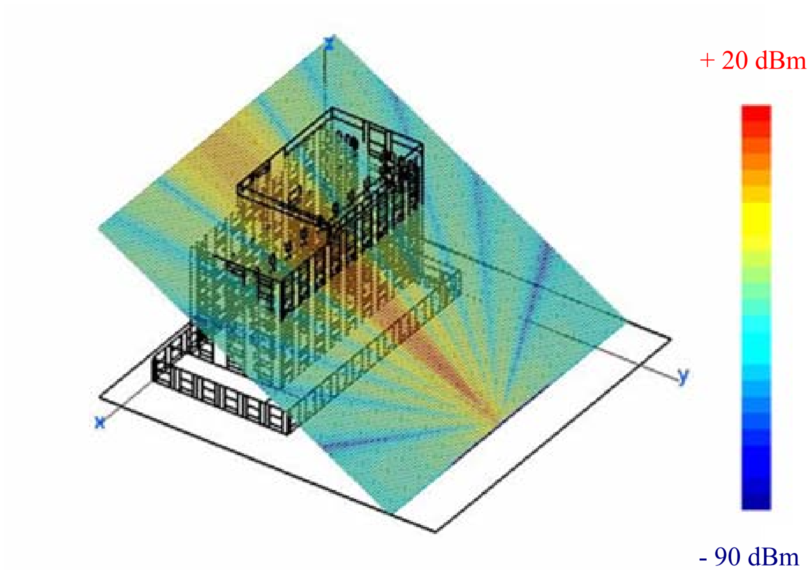

Figure 22. The plot of tilted jammer antenna radiation pattern

C. OBSERVATION PLANE

The previous chapter explains that **Urbana** requires a set of observation points at which the electric field is to be computed. The observation point file can be created either by ***bobv.x*** or a **Matlab** code. For this research, a **Matlab** script file was run and the output file was saved in ASCII **.txt* format. Then, the **.txt* file was exported to **Urbana**. This process was done for the first floor through the tenth floor, and observation planes were created 1 meter above each floor level. For each observation plane, a step of 0.5 meter between points was used. The dimensions of each observation plane are 75 meters by 40 meters. The **Matlab** code to generate the observation plane appears in the Appendix.

D. URBANA SIMULATIONS

It obvious that the indoor environment is very dynamic when WLANs are considered. Especially, people and their movements, the movement of objects, the usage of personal electronic devices that interfere with the WLAN, and the opening and closing

windows and doors will affect the signal distribution in an indoor environment. For this reason, a fixed picture of the building model is used to develop an approximation of the signal distribution.

For the simulations, a high-fidelity model with closed windows is studiedThe internal doors are considered open for all cases.

1. High-Fidelity Model

First, the building model is considered with the realistic materials described in Table 2. The power of the transmitting antenna is a fixed value of 100 mW. The input parameters and the values for the **Urbana** input file are shown in Table 4.

Input Parameters	Response Values
Input file	model#real.ur_input
Facet file	modelfinal.facet
Edge file	model0136.edge
Observation plane file	obv#.txt
Antenna type	$\lambda / 2$ omni-directional dipole
Antenna power (W)	1 (linear value for calculation)
Antenna polarization	vertical
Antenna frequency	2.4 GHz
Antenna coordinates (x,y,z)	30.0, 15.0, 16.9 (meters)
Propagation mechanism	GO
Edge diffraction	Yes (UTD)
Ray angular intervals (degree)	2
Max ray bounces	10
Coating materials	ICOAT= 0, 1, 2, 4, 6 (as described in Table 2)

Table 4. Input parameters for the high-fidelity model with closed windows

After running **Urbana** for the each observation plane, the *model#real.field* file is generated for the post processing. The command *f2f* is used to convert the *field* file to the *facet* file to view the signal distribution in **XCell**. The input parameters and the response values for the *f2f* command are shown in Table 5.

Input Parameters	Response Values
Type of E-field	Magnitude of Etot
Number of files	1
Name of field file	model#real.field
Antenna power level (W)	0.1
Histogram interval (dB)	10
Min. and Max. clip (dBm)	-200, +30
Min. and Max. range (dBm)	-90, +20
Number of levels	25
Coating code of the lowest level	1
Name of output facet file	model#realout.facet
Side of sample footprint square (meter)	0.5
Shift footprint according to z-data	Yes
Enter z-offset of footprint	0

Table 5. Input parameters and response values for *f2f* command for high-fidelity model

Figures 23 through 32 show the signal contours for the high fidelity building model with closed windows.

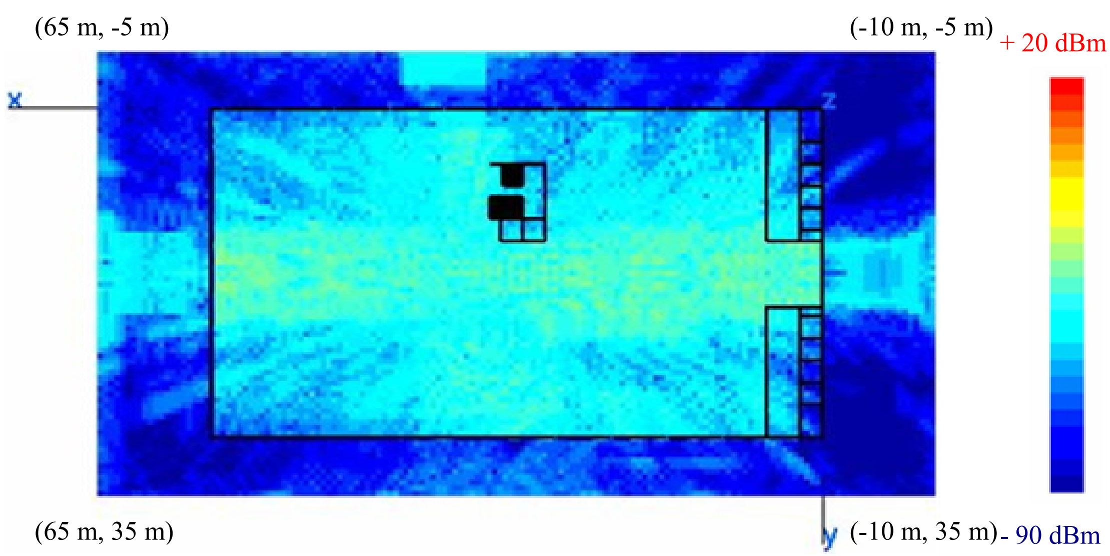

Figure 23. WLAN signal contours for the first floor for the parameters in Tables 4 and 5

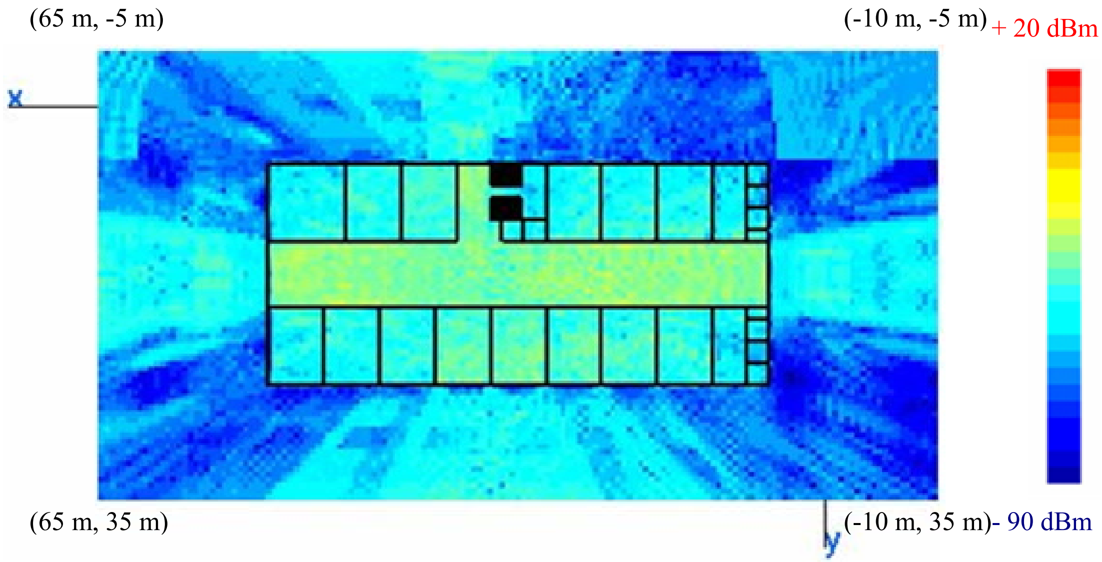

Figure 24. WLAN signal contours for the second floor for the parameters in Tables 4 and 5

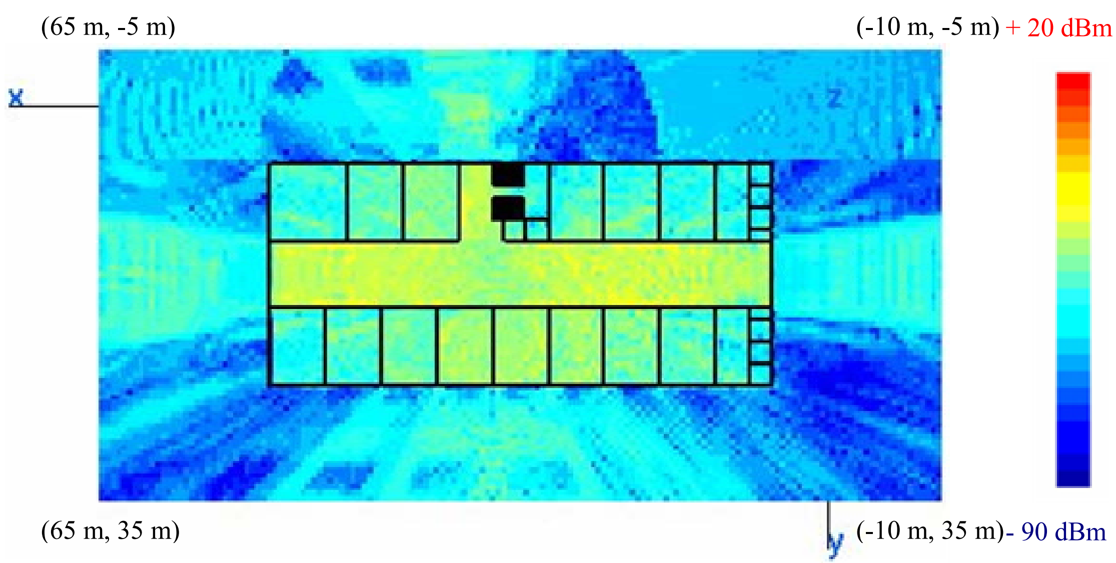

Figure 25. WLAN signal contours for the third floor for the parameters in Tables 4 and 5

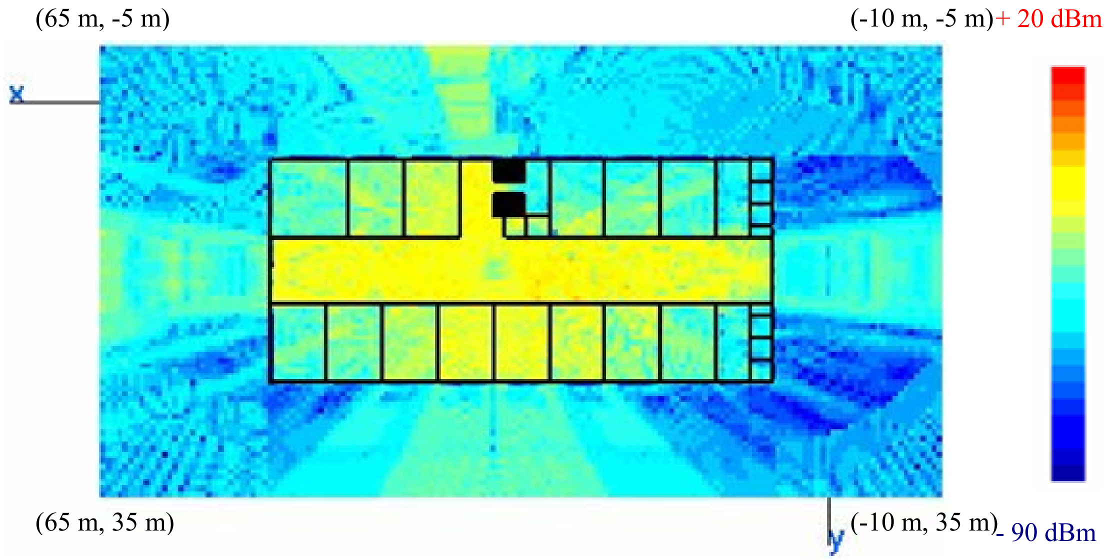

Figure 26. WLAN signal contours for the fourth floor for the parameters in Tables 4 and 5

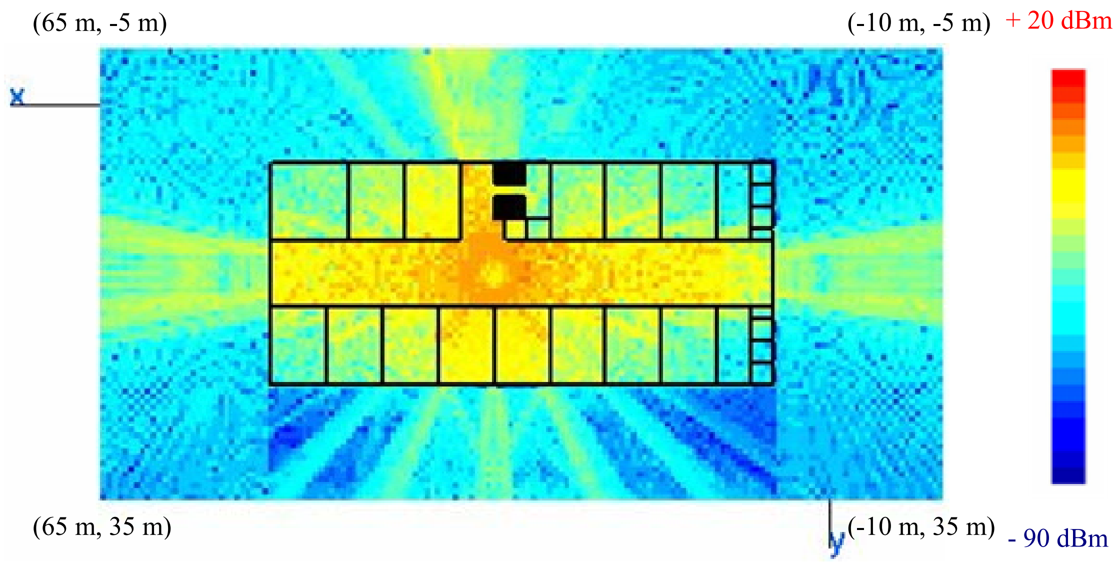

Figure 27. WLAN signal contours for the fifth floor for the parameters in Tables 4 and 5

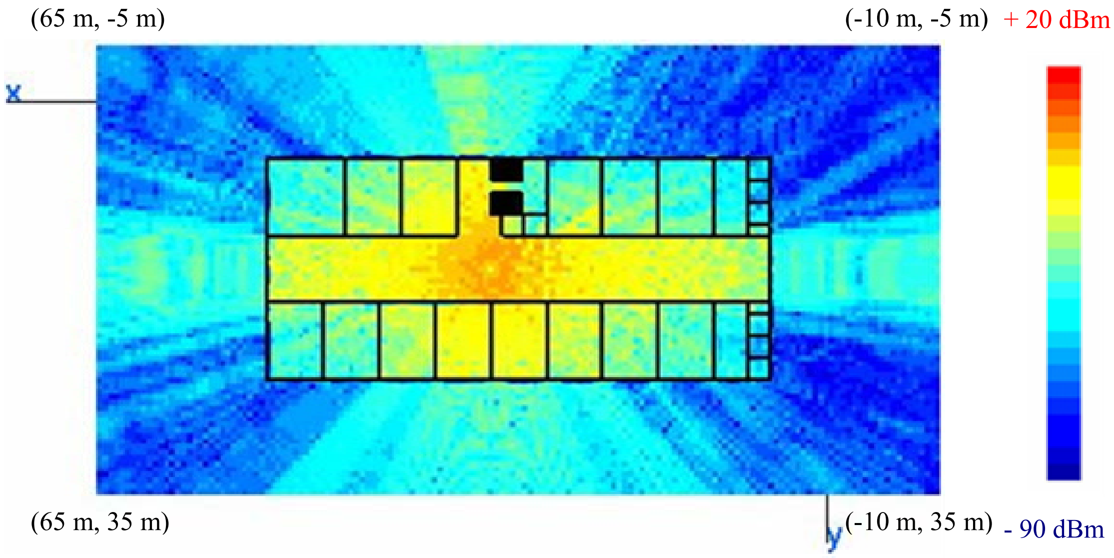

Figure 28. WLAN signal contours for the sixth floor for the parameters in Tables 4 and 5

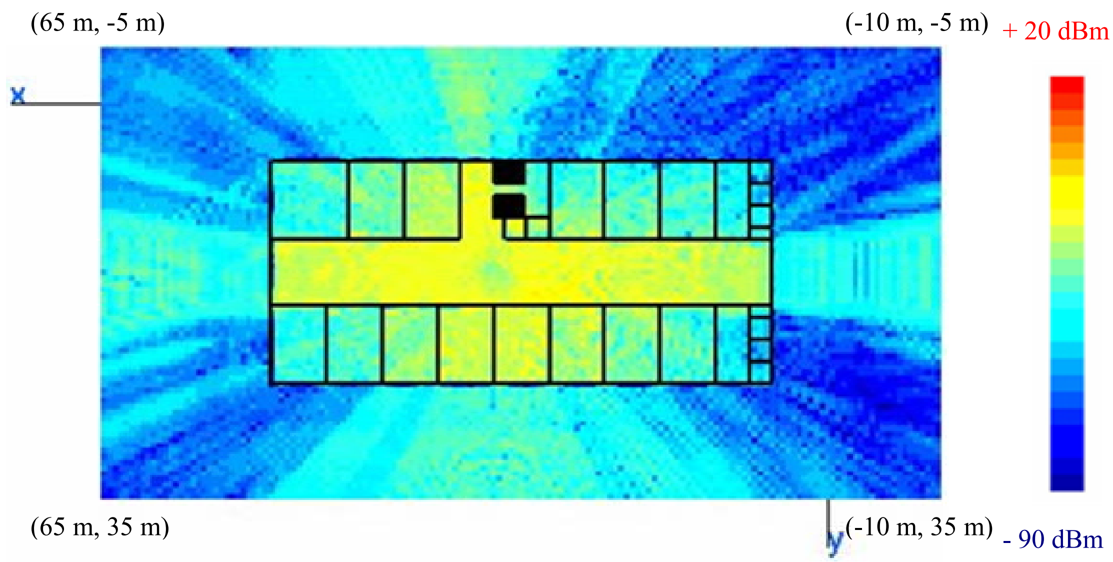

Figure 29. WLAN signal contours for the seventh floor for the parameters in Tables 4 and 5

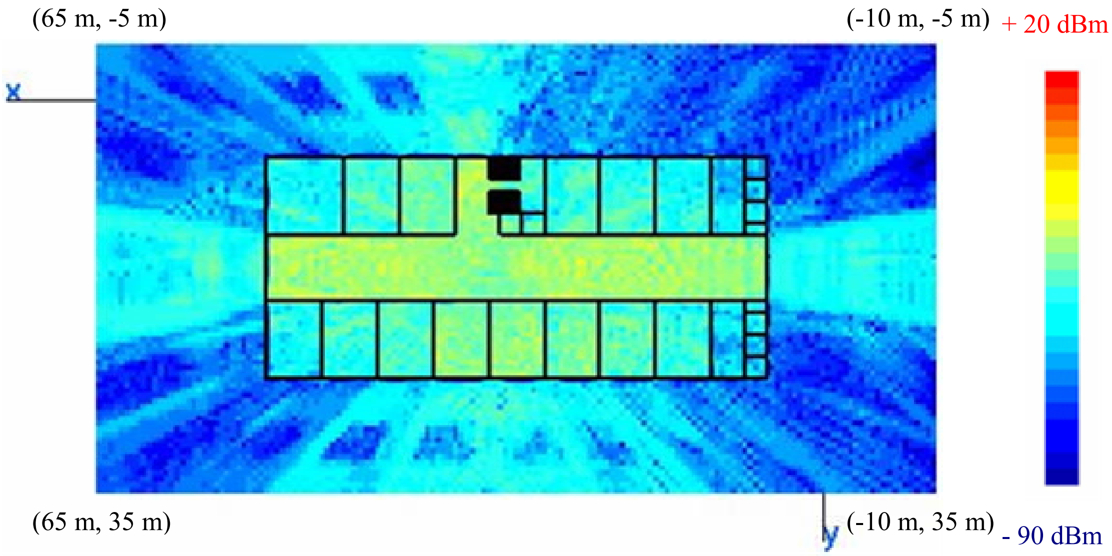

Figure 30. WLAN signal contours for the eighth floor for the parameters in Tables 4 and 5

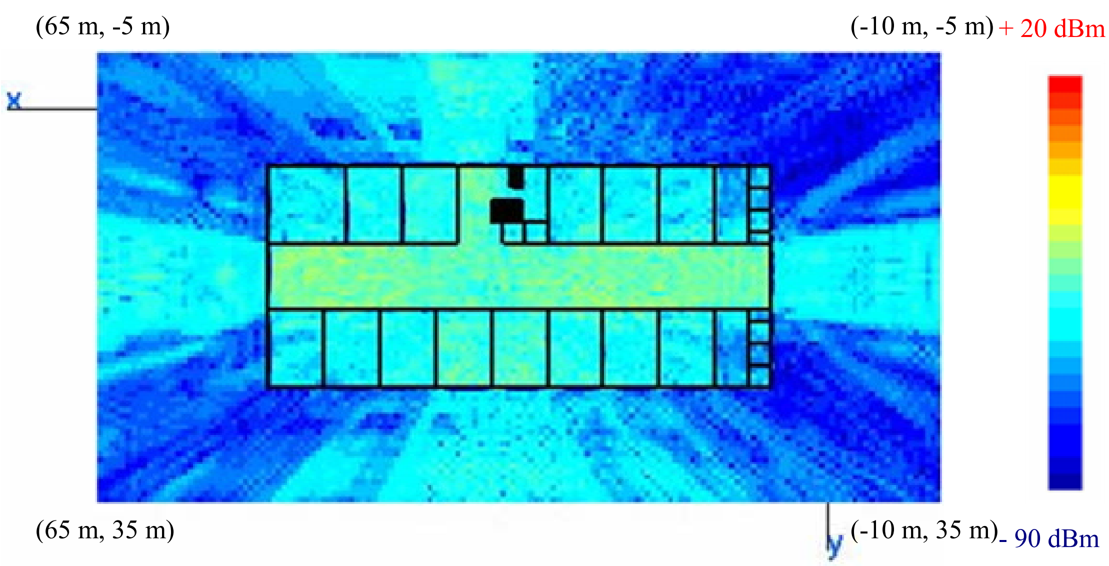

Figure 31. WLAN signal contours for the ninth floor for the parameters in Tables 4 and 5

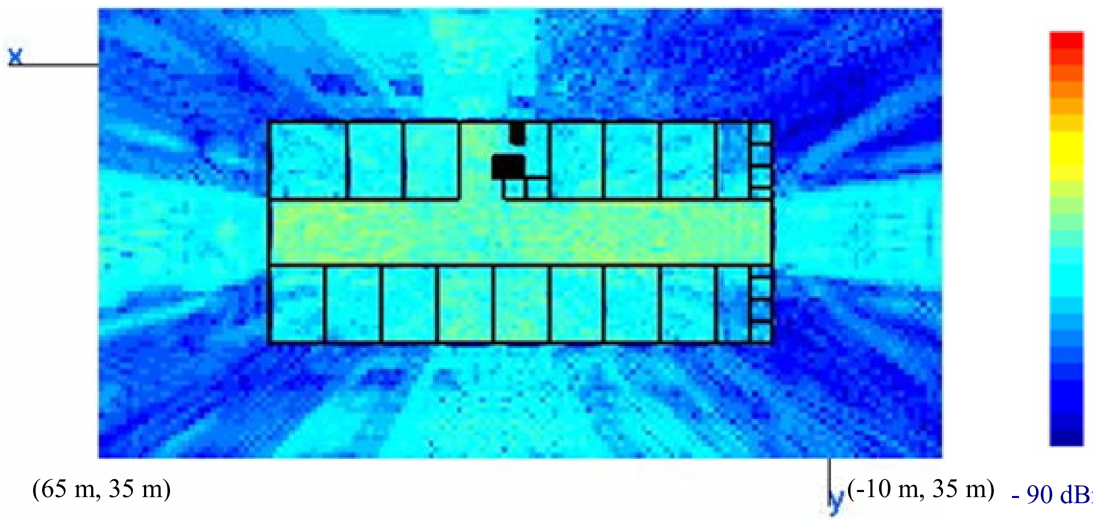

Figure 32. WLAN signal contours for the tenth floor for the parameters in Tables 4 and 5

As shown in Figures 23 through 32, the plots are scaled from -90 dBm to +20 dBm. The reason for this is to make the signal distribution for each floor more understandable. Also, a typical receiver sensitivity for 802.11g is 11 Mbps at -90 dBm [21]. The results of the 10 simulations are summarized in Table 6. The maximum and minimum signal levels at each observation plane inside the boundary of the building were calculated for the 100 mW transmitter.

Floor	Minimum Signal Level (dBm)	Maximum Signal Level (dBm)
1	- 253.57	- 28.13
2	- 105.99	- 20.61
3	- 99.96	- 13.11
4	- 102.86	- 5.57
5	- 92.02	+ 5.34
6	- 200.00	+ 1.37
7	- 200.00	- 10.40
8	- 200.00	- 18.13
9	- 200.00	- 23.72
10	- 200.00	- 29.33

Table 6. Maximum and minimum signal level at each floor with a WLAN transmitter power of 100 mW

The minimum and maximum signal levels for the fifth floor are –92.02 dBm and +5.34 dBm. When comparing the maximum signal levels, the reason the loss at the sixth floor is less than at the fourth floor is due to the location of the transmitter. Since the transmitter is located at the ceiling of the fifth floor, the observation plane at the sixth floor is closer to the transmitter than the observation plane at the fourth floor.

2. Jammer Effects on the High-Fidelity Model

The second set of simulations was run with the jammer radiating in the presence of the high-fidelity building model. The properties of the jammer were described in detail in Section B of this chapter. Tables 7 and 8 show the input parameters and response values for **Urbana** input file and for the *f2f* command.

Input Parameters	Response Values
Input file	jammer10tilt#.ur_input jammer20tilt#.ur_input jammer30tilt#.ur_input
Facet file	modelfinal.facet
Edge file	model0136.edge
Antenna file	jammer#.antenna
Radiation pattern file	jammer#.dat
Observation plane file	obv#.txt
Antenna type	10° HPBW directional 20° HPBW directional 30° HPBW directional
Antenna power	1 (linear value for calculation)
Antenna polarization	vertical
Antenna frequency	2.4 GHz
Antenna coordinates (x,y,z)	30.0, 60.0, 1.0 (meters) and tilted 30° up
Propagation mechanism	GO
Edge diffraction	Yes (UTD)
Ray angular intervals (degree)	2
Max ray bounces	10
Coating materials	ICOAT= 0, 1, 2, 4, 6 (as described in Table 2)

Table 7. Input parameters for the jammer against the high-fidelity model

Input Parameters	Response Values
Type of E-field	Magnitude of Etot
Number of files	1
Name of field file	jammer10tilt#.field jammer20tilt#.field jammer30tilt#.field
Antenna power level (W)	10 and 100
Histogram interval (dB)	10
Min. and Max. clip (dBm)	-200, +30
Min. and Max. range (dBm)	-90, +20
Number of levels	25
Coating code of the lowest level	1
Name of output facet file	jammer10tilt#.facet jammer20tilt#.facet jammer30tilt#.facet
Side of sample footprint square (meter)	0.5
Shift footprint according to z-data	Yes
Enter z-offset of footprint	0

Table 8. Input parameters and response values for *f2f* command for the jammer

The results of the simulations for the fifth floor are summarized in Table 9. When the power of the jammer is increased by a factor of ten, the minimum and the maximum signal level for either case increases 10 dB, as expected.

Jammer	Power (W)	Minimum Signal Level (dBm)	Maximum Signal Level (dBm)
10° HPBW	10	- 88.49	+ 14.13
	100	- 78.48	+ 24.13
20° HPBW	10	- 90.48	+ 15.20
	100	- 80.48	+ 25.20
30° HPBW	10	- 82.09	+ 13.01
	100	- 72.09	+ 23.01

Table 9. Maximum and minimum signal levels on the fifth floor for the jammer with three different HPBWs, and two different power levels

3. Signal-to-Jam Ratio

After running simulations for both the WLAN and jammer independently, the *f2fd* command is then used to obtain the differential signal distribution, i.e., signal-to-jam ratio (SJR) for observation points on the fifth floor. The *f2fd* command can only be run by using the same observation plane file for both *field* files. The input parameters and the response values for the *f2fd* command are shown in 0. Each time the *model5real.field* file is entered on the positive (+) side, while the *jammer#.field* file, on the other hand, is entered on the negative (-) side. This is in accordance with the definition of SJR in Equation (2.33). The zero point for the power difference is the burn-through condition. If the power difference is greater than zero (red areas), then it is said that there is sufficient available signal for the receivers on that particular observation plane to establish and maintain the link.

Input Parameters	Response Values
Type of E-field	Magnitude of Etot
Take absolute value of dB difference	No
Number of field files on (+) side	1
Name of field file on (+) side	model#real.field
Antenna power level scale factor	0.1
Number of field files on (-) side	1
Name of field file on (-) side	jammer10tilt#.field jammer20tilt#.field jammer30tilt#.field
Antenna power level scale factor	10 or 100
Histogram interval (dB)	100
Min. and Max. clip (dBm)	- 100, + 100
Min. and Max. range (dBm)	- 100, + 100
Number of levels	2
Coating code of the lowest level	1
Name of output facet file	m#j10.facet m#j20.facet m#j30.facet
Side of sample footprint square (meter)	0.5
Shift footprint according to z-data	Yes
Enter z-offset of footprint	0

Table 10. Input parameters and the response values for the *f2fd* command

The results are shown in Figures 33 through 38. Each figure shows the WLAN signal distribution, the jammer signal distribution, and the SJR. Only data for the fifth floor is shown, since this is the intended coverage area of the WLAN.

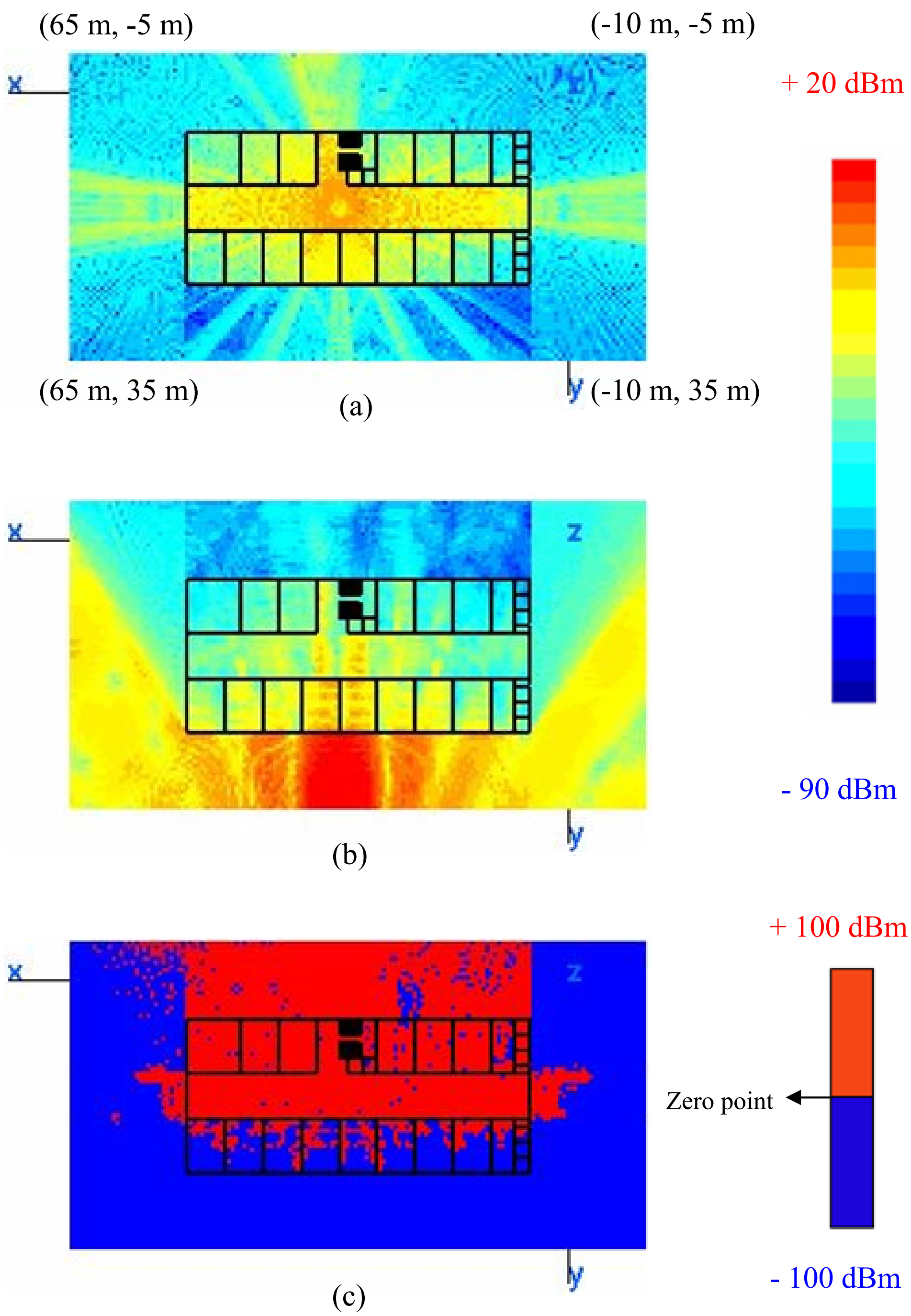

Figure 33. Signal contours for the fifth floor (a) 100 mW WLAN transmitter, (b) 10 W jammer with 10° HPBW, (c) Signal-to-jam ratio (SJR)

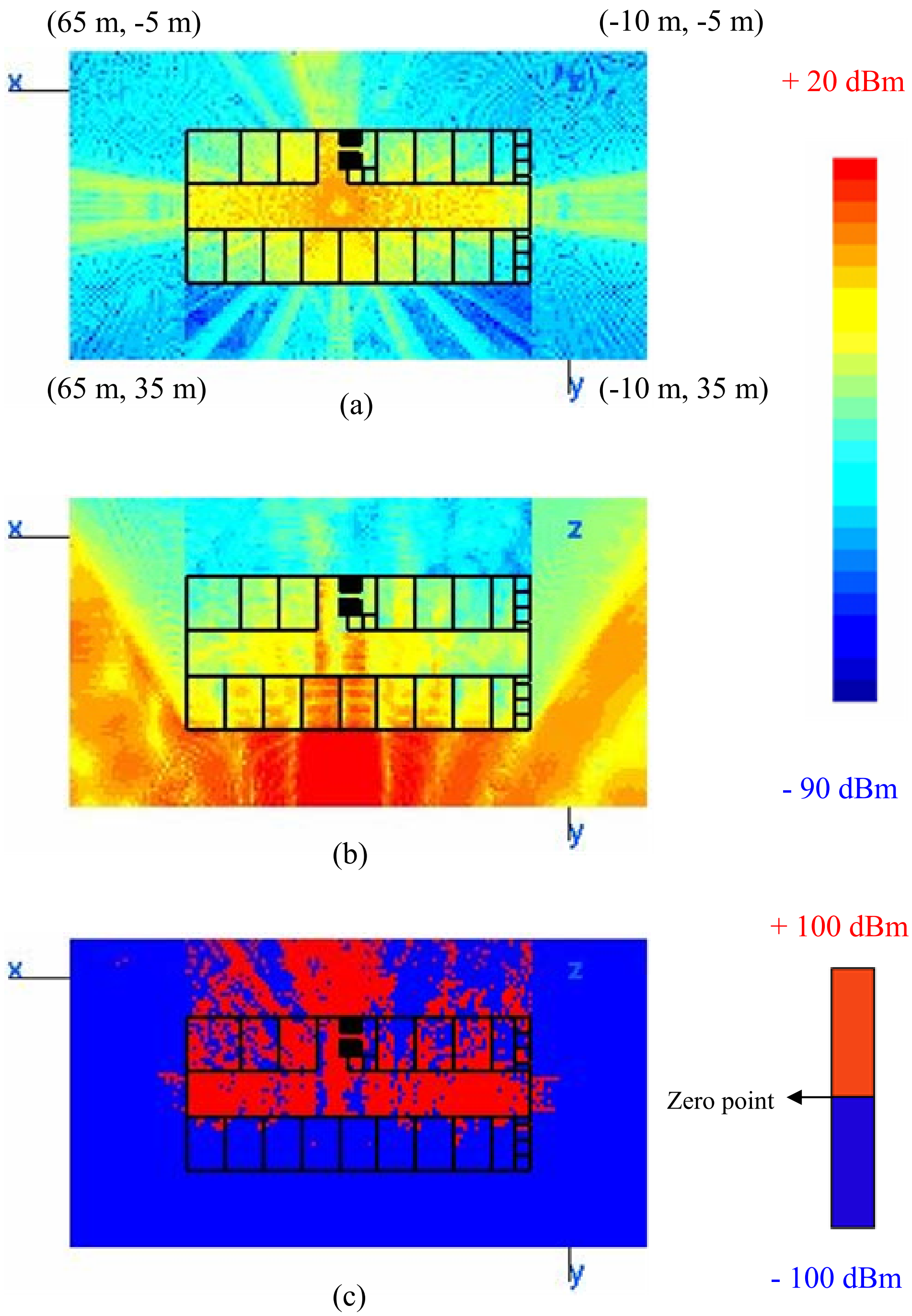

Figure 34. Signal contours for the fifth floor (a) 100 mW WLAN transmitter, (b) 100 W jammer with 10° HPBW, (c) Signal-to-jam ratio (SJR)

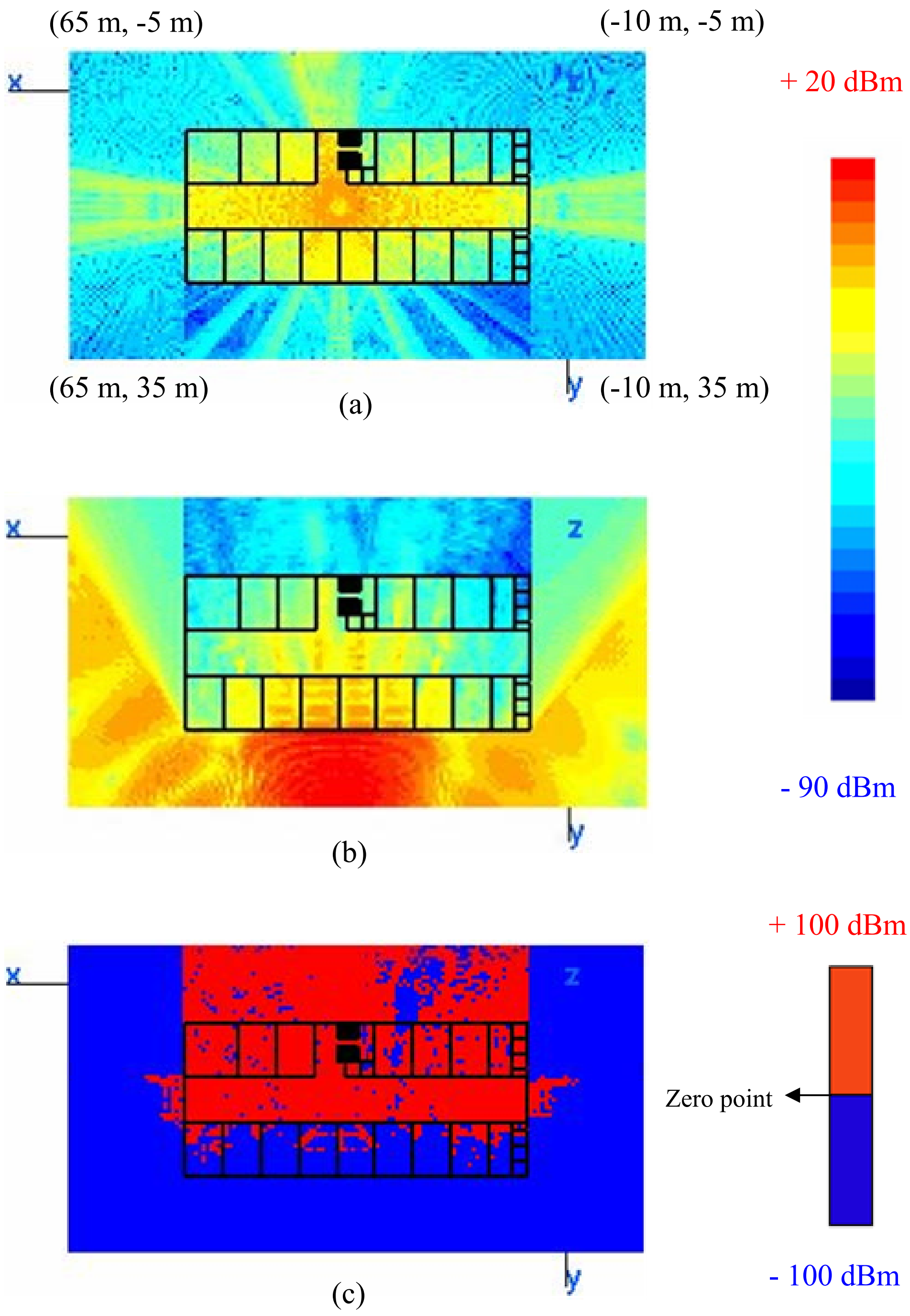

Figure 35. Signal contours for the fifth floor (a) 100 mW WLAN transmitter, (b) 10 W jammer with 20° HPBW, (c) Signal-to-jam ratio (SJR)

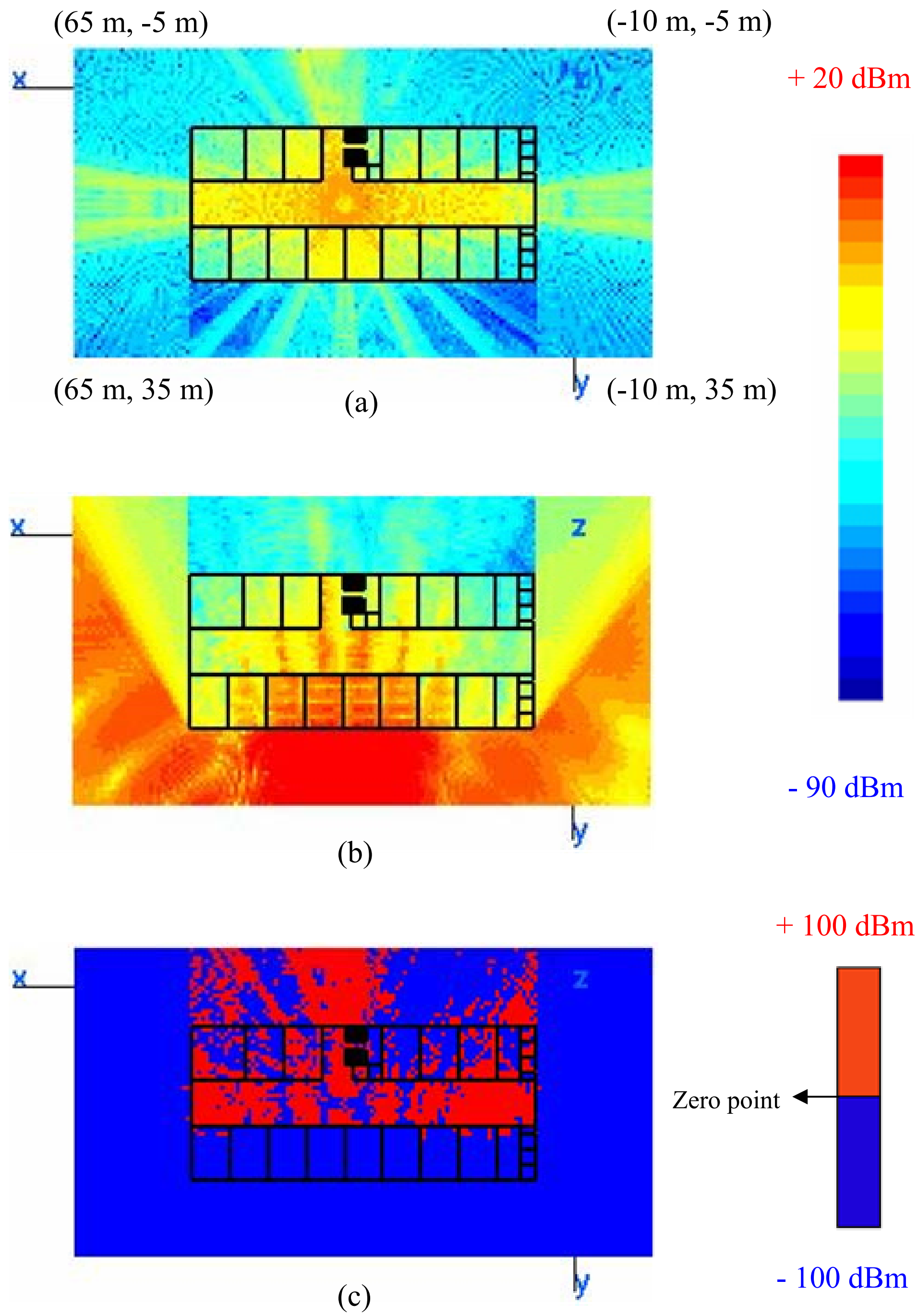

Figure 36. Signal contours for the fifth floor (a) 100 mW WLAN transmitter, (b) 100 W jammer with 20° HPBW, (c) Signal-to-jam ratio (SJR)

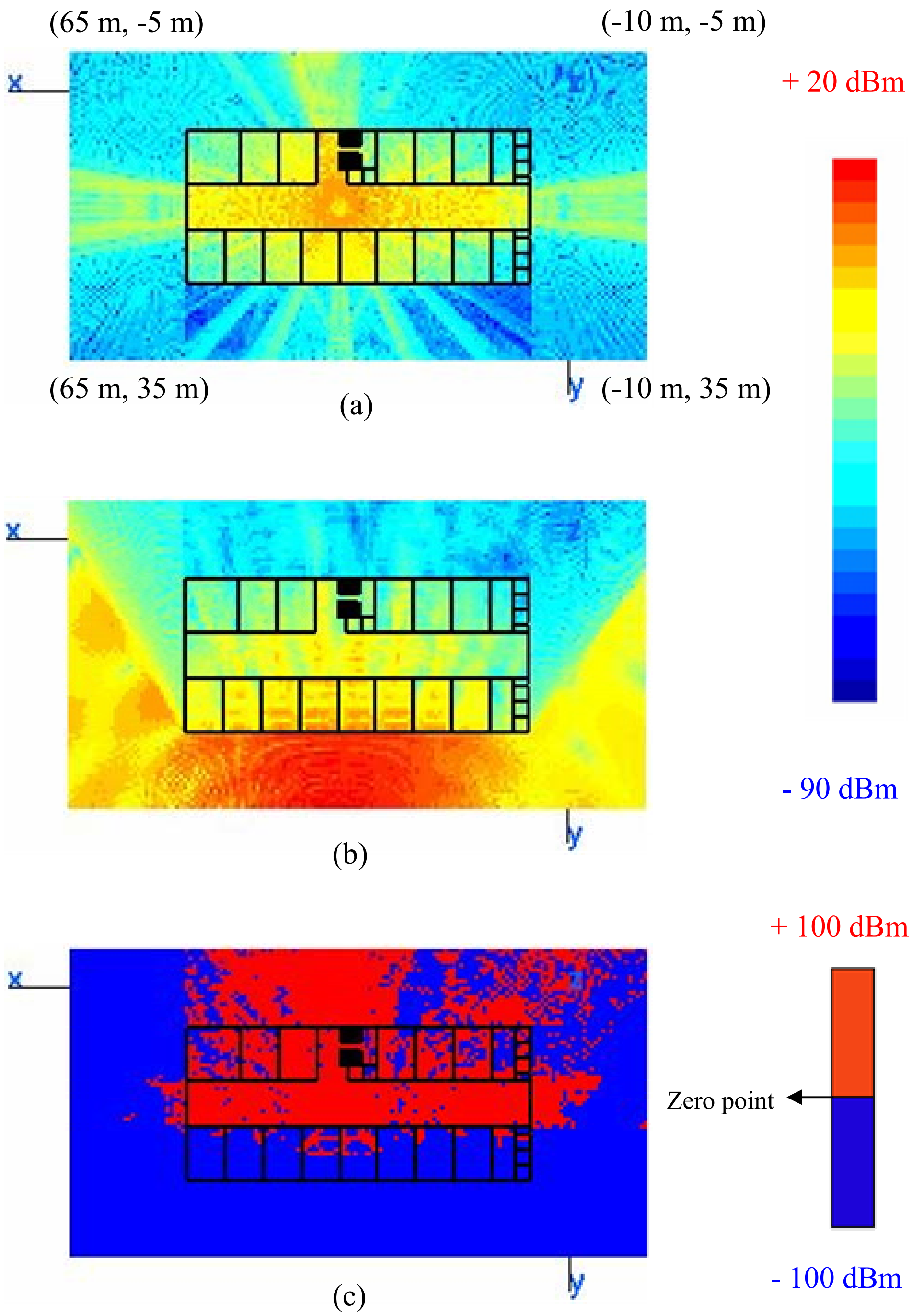

Figure 37. Signal contours for the fifth floor (a) 100 mW WLAN transmitter, (b) 10 W jammer with 30° HPBW, (c) Signal-to-jam ratio (SJR)

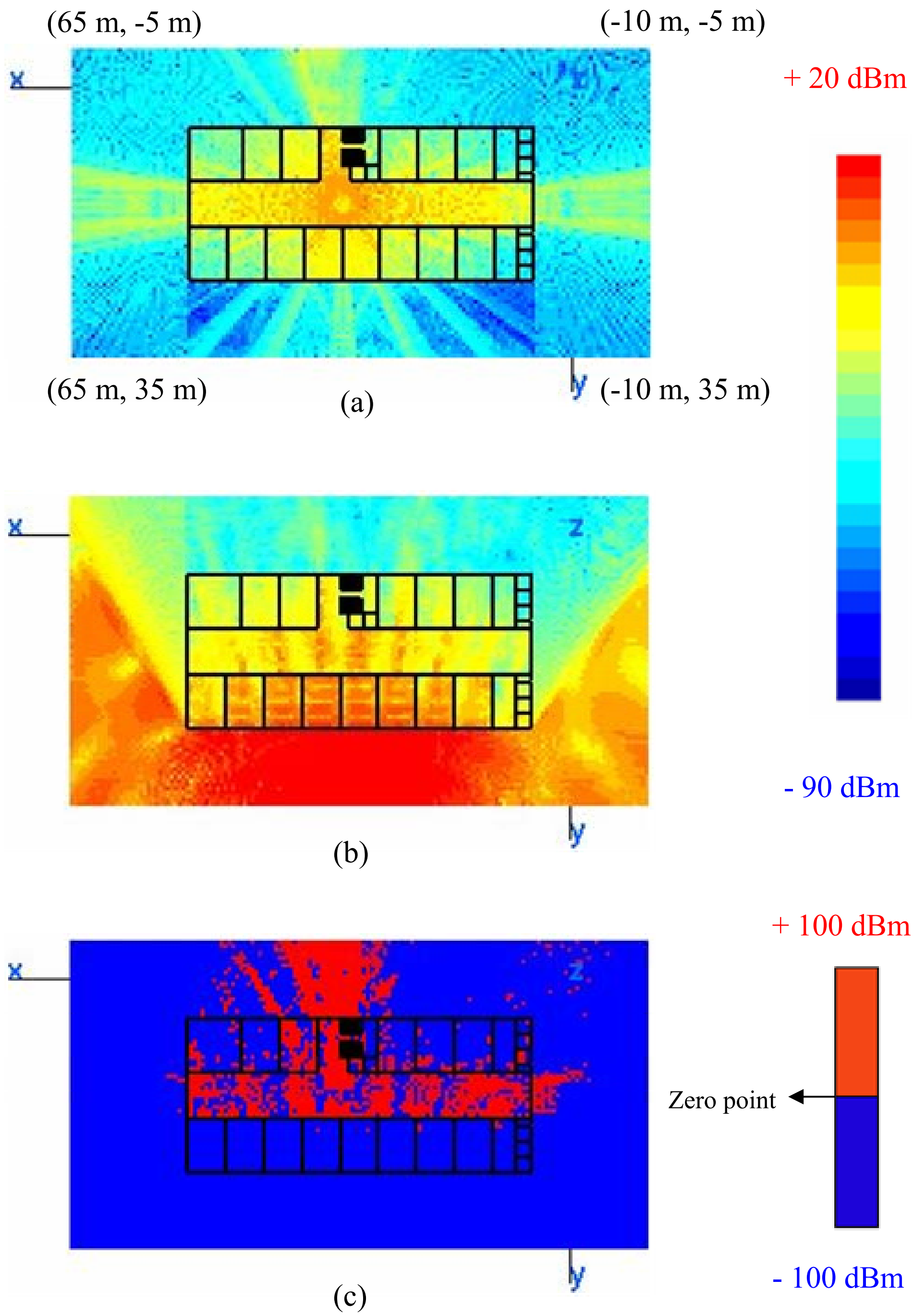

Figure 38. Signal contours for the fifth floor (a) 100 mW WLAN transmitter, (b) 100 W jammer with 30° HPBW, (c) Signal-to-jam ratio (SJR)

As shown in Figures 33 through 38, for all cases, the jammer mostly affects the rooms closest to the jammer. In part (b) of each figure, due to the shadow regions at the corner of the building, the jammer effect decreases rapidly. The rooms on the far side of the building are less affected when the jammer is 10 W. When the power of the jammer is increased to 100 W, the available WLAN signal area then obviously decreases on both sides of the building. In order to quantify the results, the number of blue and red points are calculated and written as a percentage. The percentage value of the available signal in part (c) of each figure is also tabulated. Table 11 shows the results of the simulations.

Floor	**Jammer**		**Power Difference (dB)**		**# of Points**		**Available Signal in the Area**
	HPBW	Power (W)	Min	Max	(-) Side	(+) Side	
5	10°	10	-81.53	64.79	1026	2705	72.50%
		100	-91.53	54.79	1917	1814	48.62%
	20°	10	-82.55	54.93	1250	2481	66.50%
		100	-92.55	44.93	2196	1535	41.14%
	30°	10	-80.10	54.41	1532	2199	58.94%
		100	-90.10	44.41	2598	1133	30.37%

Table 11. The results of the *f2fd* command for the fifth floor

The percentage values in Table 11 show that as either the HPBW or the power of the jammer increases, the available WLAN signal in the area decreases. The results for the variations in HPBW and power are illustrated in Figure 39. The **Matlab** code to plot Figure 39 appears in the Appendix.

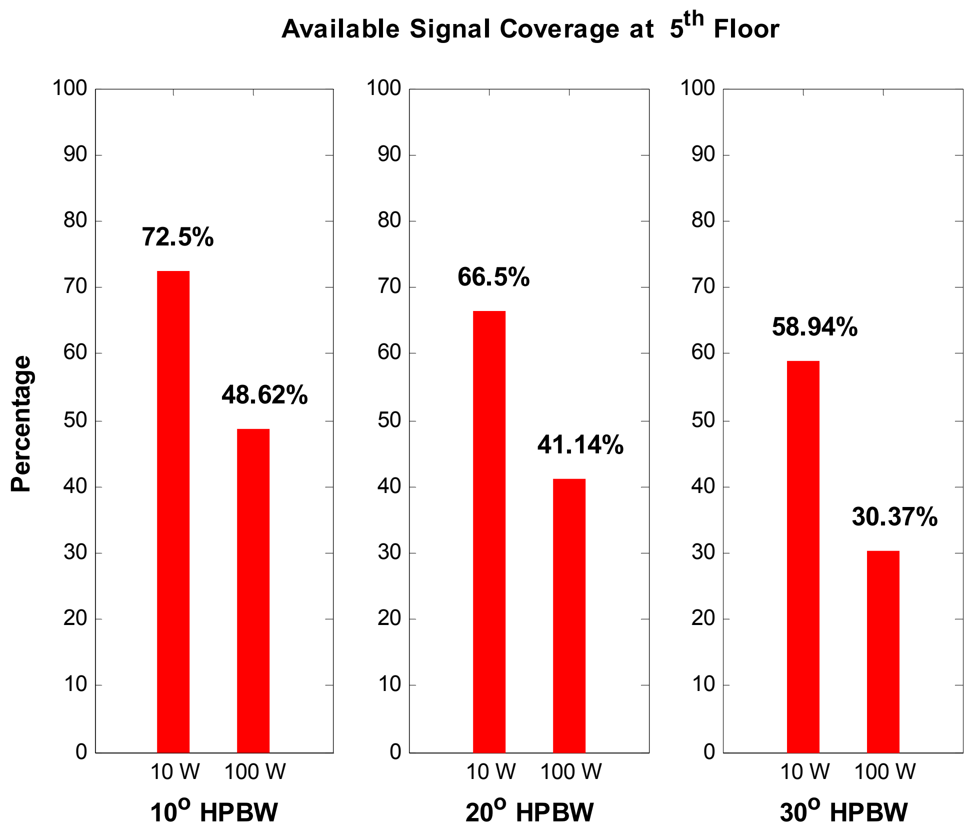

Figure 39. The effects of different HPBWs and power levels for the fifth floor

E. SUMMARY

This chapter began with the description of the WLAN transmitting antenna, the jammer and the observation plane, and then proceeded to study the simulations. The simulations were conducted for three scenarios. First, the signal distribution of a 100 mW WLAN transmitting antenna was examined for all floors. Then, the jammer effects, including three different HPBWs with two different power levels, were examined only for the fifth floor. Finally, the signal-to jam ratio (SJR) was computed for the fifth floor. The results for other floors are tabulated and shown in the Appendix. The next chapter includes a summary, conclusions, and recommended future work relating to this research.

THIS PAGE INTENTIONALLY LEFT BLANK

V. CONCLUSIONS AND RECOMMENDATIONS

A. SUMMARY

The primary objective of this thesis was to investigate the performance of wireless local area networks (WLANs) in an indoor environment with the presence of noise jamming and calculate the signal-to-jam ratio (SJR) in a high-rise building. The high-rise building model was developed with the **Rhino** software and the **Urbana** software was used to calculate the signal levels for the simulations. Specifically, the frequency of 2.4 GHz was studied. In order to make the entire building physically secure, a low power (100 mW) WLAN transmitter was located at the ceiling of the fifth floor. The jammer was located 30 meters away from the building in the parking area. The real conditions were considered for the simulations and SJR was only calculated for the area inside of the high-fidelity building model. The results indicate that increasing either the HPBW or the power of the jammer reduces the available WLAN signal.

B. CONCLUSIONS

The **Urbana** software is very useful tool for modeling wireless signal distribution for indoor environments. Signal coverage and losses can be analyzed easily, and the effectiveness of the WLAN can be optimized by running **Urbana** simulations. If the signal coverage exceeds the area where needed, i.e., WLAN signals propagate from the inside of the building to the outside, some receivers with high sensitivities might intercept the leaking WLAN signals. With the help of simulations, the security posture of the WLAN can be improved as follows,

- decreasing the power of the WLAN transmitter,
- increasing the sensitivity of the access point and the receivers,
- locating the transmitting antenna in the most interior part of the building, and
- using directional antennas to limit the signal distribution.

If the WLAN signal is not interceptable due to limited coverage and physical security, then the alternative is to jam the signal. The effectiveness of the jammer depends on,

- the distance to the WLAN coverage area,
- the power of the jammer transmitter,
- the radiation pattern of the jammer antenna,
- the material properties of the building, and
- the openings of the building.

C. FUTURE WORK

The present research was only concerned with calculating SJR for a single WLAN transmitter versus a single jammer. Future work might entail,

- analyzing the SJR for multiple WLAN transmitters versus multiple jammers,
- comparing the effects of different placements of the transmitters, such as placing the jammer inside the building.
- analyzing the effects of different polarizations of the WLAN transmitter antenna and the jammer antenna,
- analyzing the SJR by using different types of antennas,
- analyzing the effects of different material properties, such as using PEC materials for the outer walls, and
- calculating the jam-to-signal ratio (JSR).

APPENDIX

The appendix includes a sample **Urbana** input file with and *antenna* file, Matlab codes for the jammer antenna, the observation points file and the SJR. Finally, the tabulated values and the plots are also included for the other floors.

A. SAMPLE URBANA INPUT FILE AND ANTENNA FILE

```
--- input Urbana v 2.5-----------------------------------------------
#
# ********************************
# A---scatterer file,length & freq
# ********************************
#--- name of scatterer file in ACAD format (e.g. wall.facet)
modelfinal.facet
#--- length unit:1=inch, 2=cm, 3=meter, 4=mm, 5=mil
3
#--- uniform freq (GHz): start freq, end , nstep
#    (nstep=0 means: just do first freq. CAUTION: antenna patterns are
#     assumed to be indep. of freq and is calculated at end freq)
2.4 2.4 0
#
# *********************************
# B--- Antenna Description and List
# *********************************
#
#---Enter method of describing antennas.
#   (1 = here, 2 = file):
2
#---If described in file, enter file name:
jammertilt.antenna
#---If described here, fill in sections B1, B2, B3.
#   If described in file, use dummy data in sections B1, B2, B3
#   (specify one dummy antenna type, dummy antenna origin,
#    and one dummy item in antenna list).
#
# ***********************
# B1: Define Antenna Types
# ***********************
#
#   Two lines for each type.
#     Line1: type ID, ant code
#     Line2: parameters
#
#   Type ID must start from 1 and increment by 1 thereafter
#
#   Ant Code   meaning            parameters
#   --------   ----------------   -----------------------------
#      1       pattern file       filename(ascii)
#      2       dipole             length(real)
#
#   Antenna Types list:
#
#   Enter number of antenna types:
1
#   Type #1
1 1
0.0625
#
# *********************************************
# B2: Enter origin of antenna coord in main coord
# *********************************************
#
0.0 0.0. .0
#
```

```
# **********************
# B3: Create Antenna List
# **********************
#
#   Three lines for each antenna.
#     Line1: Type ID, location (x,y,z), power (watts), phase(deg)
#     Line2: Local x-axis in main coord.
#     Line3: Local z-axis in main coord.
#
#   Enter number of antennas:
1
#
#   Antenna #1
1  30.0 60.0 1.0  1 0
-1. 0.5 0.8660
0. -0.8660 0.5
#
# *********************
# C---Observation points
# *********************
#--- Observation points defined with respect to main coord. system 7.
#    Enter method of specifying list of points.
#    (1 = here, 2 = file):
2
#--- If points are listed here, enter number of points (kobtot):
1
#--- If listed here (1 above), List xyz of points in main coord 7
#    (one point at a line). If 2 above, include one dummy line.
1.           2.               -11.00
#--- If points listed in file (2 above), enter name of file.
obv5.txt
#--- Include direct Tx to observer contribution.
#    If you turn on the direct contribution from the transmitter to the
#    observation point, computed result will be the total field, which is
#    the incident + scattered field.   For propagation analysis, this is
#    the preferred setting.  Otherwise, the result only includes the
#    scattered field.
#
#    Include direct contribution from transmitter to observation point (rx)
#    (1 = yes, 0,2 = no):
1
#--- Compute received power into Rx antenna.
#    Urbana always computes field levels at the observation point.
#    If you specify an Rx antenna, Urbana will also compute the received
#    power and record the results in the (runname).couple file.
#    This causes a moderate but slow-down when using the SBR method (below).
#
#    Include Rx antenna (1 = yes, 0,2 = no):
0
#--- Rx antenna specification
#    Remaining entries in Section C can be ignored if not including
#    an Rx antenna.
#    Enter antenna type (1 = pattern file, 2 = dipole):
2
#    Each antenna type requires additional parameters.
#    List of expected parameters follows.  Choose one.
#
#    Type  Description     Expected Parameter(s)
#    1     Pattern File    File Name (e.g., beam.antpat)
#    2     Dipole          Length (in prevailing unit)
#
#    Enter parameter(s) on next line:
2.5
#--- Rx antenna orientation
#    Enter local x-axis of Rx in global coordinates
1. 0. 0.
#    Enter local z-axis of Rx in global coordinates
0. 0. 1.
#
# ****************************
# D---Theoretical consideration
# ****************************
```

```
#--- Choose method of computation
#    0 = compute fields in the ABSENCE of the scatterer
#    1 = compute fields by SBR
#    2 = compute fields by GO
2
#--- If SBR, select a PO integration scheme at bounce points
#    1 = do integration at first & last bounce points only
#    2 = do so at all bounce points (GTD formulation)
#    3 = do so at all bounce points (PTD formulation)
2
#--- Edge diffraction
#    SBR can be enhanced with PTD edge diffraction.
#    GO can be enhanced with GTD edge diffraction.
#    Add edge diffraction (0,2=no, 1=ILDC (SBR or GO), 3=UTD (GO only)
3
#--- If edge diffraction switched on, enter name of edge file
#    (e.g., wall.edge or dummy if edge not included).
model0136.edge
#--- Choose method of ray launch
#    1 = by (baby) facet, achieving a uniform first bounce surface density
#    2 = uniform angular distribution (burst launch)
#    (If computation by GO, must select 2 = burst launch)
2
#--- If ray launch by (baby) facet (1 above), enter ray density:
#    # rays/wavelength (normally 5-10)
5
#--- If burst ray launch (2 above), enter angular interval (deg).
#    (Typically 0.25 - 2.0 deg)
2.
#--- max permissible ray bounces (normally 5-10)
10
#--- max-voxdepth = max depth of BSP tree (normally 20)
#    max-voxl = max facets in each voxel(normally 10)
#    (Larger voxdepth & smaller voxl lead to faster ray tracing
#     but more computer memory)
20,10
#--- ICOAT for absorbing facets
888
#--- IQMATRIX for divergence factor
#     1 = calculated by Q-matrix
#     2 = ignored except for the spherical wave spread
2
#--- IF using Q-matrix, name target curvature file(e.g. wall.curv)
dummy.curv
#--- IPEC=1 if all pec,  =2 if coating present
2
#--- For PEC scatterer, give the magnitude of reflection coeff
#    (use 1.0 for ideal PEC, use less for rough PEC--fudging)
1.
#--- IF PEC, the rest coating info is dummmy
#--- material reflection is done through a look-up table
#    specify the freq interval in GHz for the table e.g. 0.25
#    (dummy if input freq less than 51)
0.2
********************
E---coating material
********************
---- number of materials
      (NOT including pec, which is identified by ICOAT=0)
      (NOT including absorbing facets:  ICOAT=28 or 888)
      (If 3 material, urbana reads only ICOAT=1-3)
6        <----NCOTOT
--- for each material, identify its boundary type:
    iboundary = 1 if impedance boundary
                2 if layered slabs with PEC backing
                3 if penetrable layered slabs with air backing
                4 if penetrable FSS Tx/Refl table supplied by user
                5 if same as 2 except using freq-dep ramlib.d
                6 if antenna refl table supplied by user
                7 if layers over semi-infinite ground
# for each material, given info by following the templates
^^^ ICOAT=1 ^^^^^^^^^^^^^^^^^^^^^^^^^^^^^^^^^^^^^^^^^^^^^^^^^^^^
```

```
--- iboundary
3
--- number of layers over air backing
    (1st layer is farthst fr incid field and innermost)
1
--- thick,epsilon(c),mu(c),resistivity(ohm)
.300 (10.1,-0.5) (1.0,-0.0) 1e30
^^^ ICOAT=2 ^^^^^^^^^^^^^^^^^^^^^^^^^^^^^^^^^^^^^^^^^^^^^^^^^^^^^^
--- iboundary
3
--- number of layers over air backing
    (1st layer is farthst fr incid field and innermost)
1
--- thick,epsilon(c),mu(c),resistivity(ohm)
.100 (10.1,-0.5) (1.0,-0.0) 1e30
^^^ ICOAT=4 ^^^^^^^^^^^^^^^^^^^^^^^^^^^^^^^^^^^^^^^^^^^^^^^^^^^^^^
--- iboundary
3
--- number of layers over air backing
    (1st layer is farthst fr incid field and innermost)
1
--- thick,epsilon(c),mu(c),resistivity(ohm)
.0250 (6.0,-0.0) (1.0,-0.0) 1e30
^^^ ICOAT=6 ^^^^^^^^^^^^^^^^^^^^^^^^^^^^^^^^^^^^^^^^^^^^^^^^^^^^^^
--- iboundary
7
--- number of layers over air backing
    (1st layer is farthst fr incid field and innermost)
1
--- thick,epsilon(c),mu(c),resistivity(ohm)
.1000 (3.0,-0.0) (1.0,-0.0) 1e30
---epsilon(c),mu(c) of semi-infinite ground
(3.00,-0.00) (1.00,-0.00)

(End of regular input file. Leave a few blank lines)




-----------------------------------------------------------------
'OPTIONAL ADVANCE FEATURES' (Do not change letters in quotations)
# The line above must be placed at the end of the regular urbana
# input. Advance features are designed for special applications or
# for testing codes.  They are not needed by general usages.
# -----------------------------------
# ADVANCE1: ADD GTD-TYPE BLOCKAGE CHECK
# -----------------------------------
# In regular urbana computation, blockage check is mostly done by
# PTD principle. For interior scattering in a confined region, use of
# GTD principle may be more appropriate.
# Option to use GTD principle:  1=yes,    2=no (regular case)
2
# -------------------------------------
# ADVANCE2: SIMPLE TERRAIN BLOCKAGE MODEL
# -------------------------------------
# For GO method, terrain generates 100% blockage, and blocked rays leave
# no energy behind a hill.  With this feature, LOS rays and UTD edge
# diffraction rays can pass through terrain, with some attenuation.
# Attenuation is measured in dB per hill.  Each hill is identified
# by two passages through two terrain facets.
# Can only be used with GO method (and UTD edge option).
# Use simple terrain model: 1 = yes, 2 = no (regular case)
2
# Enter coating code range of terrain facets (e.g., 1, 2):
1 1
# Enter amount of attenuation per hill (dB, > 0):
5.
# --------------------------------------------
# ADVANCE3: APPROXIMATE DOUBLE DIFFRACTION MODEL
# --------------------------------------------
# For GO + UTD method, only single diffraction is considered.
# With this feature, double diffraction is approximated by identifying
```

```
# surfaces which block the single diffraction, such as building walls.
# If one or two facets block the path from the single diffraction point
# to the transmitter, the diffraction is still included, but with attenuation.
# Works best if "diffracting facets", marked by their coating code, are
# always associated with enclosed structures with well defined edges.
# Use double diffraction model: 1 = yes, 2 = no (regular case)
2
# Encounter coating code range of diffracting facets (e.g., 5, 10):
2 2
# Enter amount of attenuation for second diffraction (dB, > 0);
10.
# ----------------------
# ADVANCE4: ACCELERATION
# ----------------------
# For large scenes, run time grows both with the number of field
# observation points and the number of edges.  Normally, all combinations
# of lit edges and observation points are considered.  This feature
# accelerates the processing by limiting the scope of considered edge
# interactions to region around the LOS path from the transmitter
# to the observation point.  For example, to run a 5 km by 5 km scene,
# one may choose a 250 m interaction radius.  For each observation
# point, edges are ignored that lie outside an ellipse whose foci are the
# Tx and the observation point and whose major axis is the LOS distance
# plus 500 m (radius x 2).
# This feature can also be used to automatically filter edge files
# whose domain far exceeds the domain of observation points.
# Only use this feature for terrestrial simulations where the scene
# is nominally parallel to the x-y plane.
#
# Use large scene acceleration: 1 = yes, 2 = no (regular case)
2
# Enter radius of interaction
250.
```

%%%

```
# ************************
# B1: Define Antenna Types
# ************************
#
#   Two lines for each type.
#     Line1: type ID, ant code
#     Line2: parameters
#
#   Type ID must start from 1 and increment by 1 thereafter
#
#   Ant Code   meaning            parameters
#   --------   ----------------   -----------------------------
#      1       pattern file       filename(ascii)
#      2       dipole             length(real)
#
#   Antenna Types list:
#
#   Enter number of antenna types:
1
#   Type #1
1 1
jammer1.dat
#
# *********************************************
# B2: Enter origin of antenna coord in main coord
# *********************************************
#
0.0 0.0. .0
#
```

```
# **********************
# B3: Create Antenna List
# **********************
#
#   Three lines for each antenna.
#     Line1: Type ID, location (x,y,z), power (watts), phase(deg)
#     Line2: Local x-axis in main coord.
#     Line3: Local z-axis in main coord.
#
#   Enter number of antennas:
1
#
#   Antenna #1
1  30.0 60.0 1.0  1 0
-1 0.5 0.8660
0 -0.8660 0.5
#
```

B. MATLAB CODES

1. Jammer Antenna Radiation Pattern File

```
% Antenna Pattern File Generation
close all;
clc;
clear;
lamda = (3*10^8)/(2400*10^6);
HPBW = 10; % in degrees
a = 58.4 * lamda / (2*HPBW) % Uniform Circular Aperture Size (radius)
beta = 2*pi/lamda;
E0 = 1;
c = j*beta*E0*pi*a^2/(2*pi); %Constant term in E field
Directivity = (4*pi*pi*a^2)/lamda^2
Directivity_dB = 10*log10(Directivity)
step1 = 90; %Vertical Steps
step2 = 180; %Horizontal Steps
d_theta = 180/(step1);
d_phi = 360/(step2);
k = 0;
ip = 0;
iq = 0;
for phi = 0:d_phi:360
for theta = 0:d_theta:180 %plots out the zero point
k = k+1;
arg=beta*a*sin(theta*pi/180);
f = 1;
if abs(arg)>=1e-5
f = 2*besselj(1,arg)/arg;
end
e_theta = cos(phi*pi/180)*c*f;
e_phi = -sin(phi*pi/180)*cos(theta*pi/180)*c*f;
if theta > 90
e_theta = 0;
e_phi = 0;
end
if phi == 0
ip = ip + 1;
et0(ip) = 20*log10(abs(e_theta));
ep0(ip) = 20*log10(abs(e_phi));
eth(ip) = theta;
```

```
end
if phi == 90
iq = iq + 1;
et90(iq) = 20*log10(abs(e_theta));
ep90(iq) = 20*log10(abs(e_phi));
eth90(iq) = theta;
end
A(k,1:4) = [real(e_theta), imag(e_theta), real(e_phi), imag(e_phi)];
end
end
save antennapat1 A -ASCII;
figure(1)
plot(eth,et0,eth,ep0)
title('Directional Antenna Pattern (HPBW=10 degrees)')
xlabel('Angle [degree]')
ylabel('Relative Power [dB]')
grid
figure(2)
plot(eth90,et90,eth90,ep90)
xlabel('Angle [degree]')
ylabel('Relative Pattern, dB')
grid
```

2. Observation Points File

```
% Observation Points
clc;
clear;

step = .5; %footprint
i = 1;
z = 15;

    for x = -10:step:65
      for y = -5:step:35
          M(i,:)=[x,y,z];
          i=i+1;
       end
   end

Lines=i-1

save observ1strip.obv M -ASCII;
```

3. Plotting the Effects of Different HPBWs and Power Levels

```
clear; clc;
width=.4;
power={'10 W', '100 W'};

x=[72.50, 48.62];
y=[66.50, 41.14];
z=[58.94, 30.37];

subplot(1,3,1)
bar(x, width, 'r', 'EdgeColor', 'r')
text(0.6,max(x)+5,['\bf',num2str(x(1)),'%'])
text(1.6,min(x)+5,['\bf',num2str(x(2)),'%'])
axis([0 3 0 100]);
```

```
set(gca,'xticklabel',power, 'FontSize', 8);
xlabel ('\bf 10^o HPBW','FontSize', 10);
ylabel('\bf Percentage','FontSize', 10);

subplot(1,3,2)
bar(y, width, 'r', 'EdgeColor', 'r')
text(0.6,max(y)+5,['\bf',num2str(y(1)),'%'])
text(1.6,min(y)+5,['\bf',num2str(y(2)),'%'])
set(gca,'xticklabel',power,'FontSize', 8);
xlabel ('\bf 20^o HPBW','FontSize', 10);
axis([0 3 0 100]);
title({'\bf   Available   Signal   Coverage   at      5^{th}   Floor','
'},'FontSize', 10);

subplot(1,3,3)
bar(z, width, 'r', 'EdgeColor', 'r')
text(0.6,max(z)+5,['\bf',num2str(z(1)),'%'])
text(1.6,min(z)+5,['\bf',num2str(z(2)),'%'])
set(gca,'xticklabel',power,'FontSize', 8);
xlabel ('\bf 30^o HPBW','FontSize', 10);
axis([0 3 0 100]);
```

C. TABULATED RESULTS AND PLOTS FOR THE OTHER FLOORS

Floor	Jammer		Power Difference (dB)		# of Points		Available Signal in the Area
	HPBW	Power (W)	Min	Max	(-) Side	(+) Side	
1	10°	10	-181.79	13.08	6718	53	0.79%
		100	-191.79	3.08	6769	2	0.03%
	20°	10	-191.51	8.57	6751	20	0.30%
		100	-201.51	-1.42	6771	0	0.00%
	30°	10	-187.57	9.77	6745	26	0.38%
		100	-197.57	-0.23	6771	0	0.00%

Table 12. The results of the *f2fd* command for the first floor

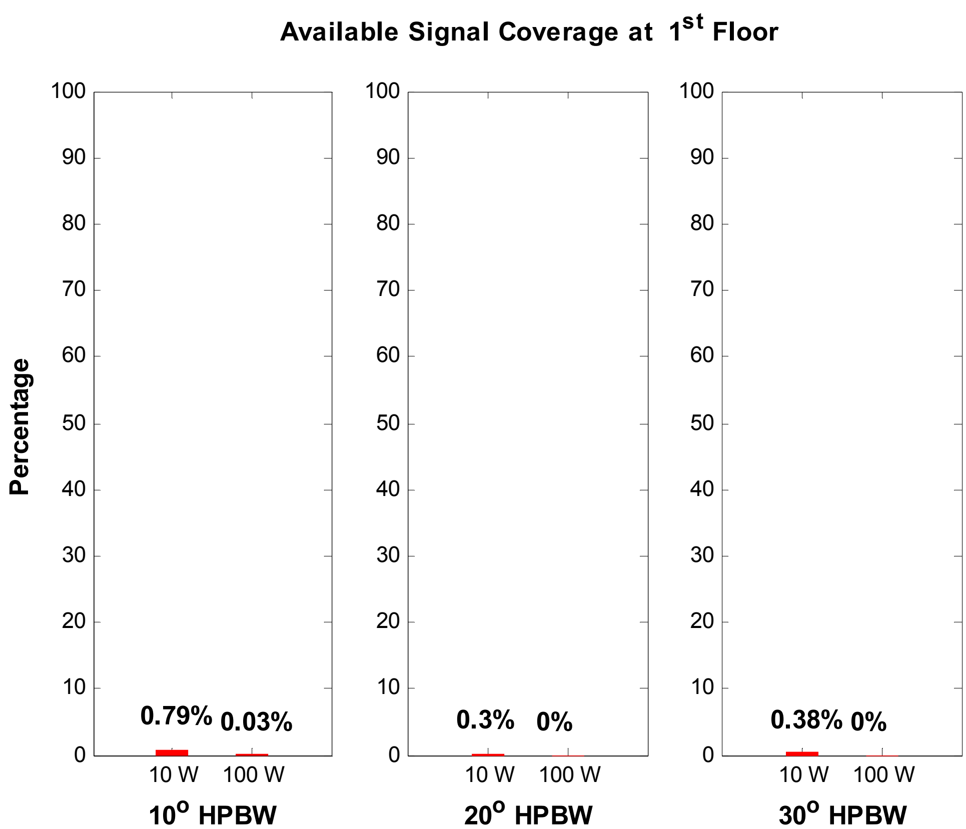

Figure 40. The effects of different HPBWs and power levels for the first floor

Floor	Jammer		Power Difference (dB)		# of Points		Available Signal in the Area
	HPBW	Power (W)	Min	Max	(-) Side	(+) Side	
2	10°	10	-73.36	31.46	2672	1059	28.38%
		100	-83.35	21.47	3461	270	7.24%
	20°	10	-75.69	32.47	2634	1097	29.40%
		100	-85.69	22.47	3478	253	6.78%
	30°	10	-83.60	31.72	3125	606	16.24%
		100	-93.60	21.72	3656	75	2.01%

Table 13. The results of the *f2fd* command for the second floor

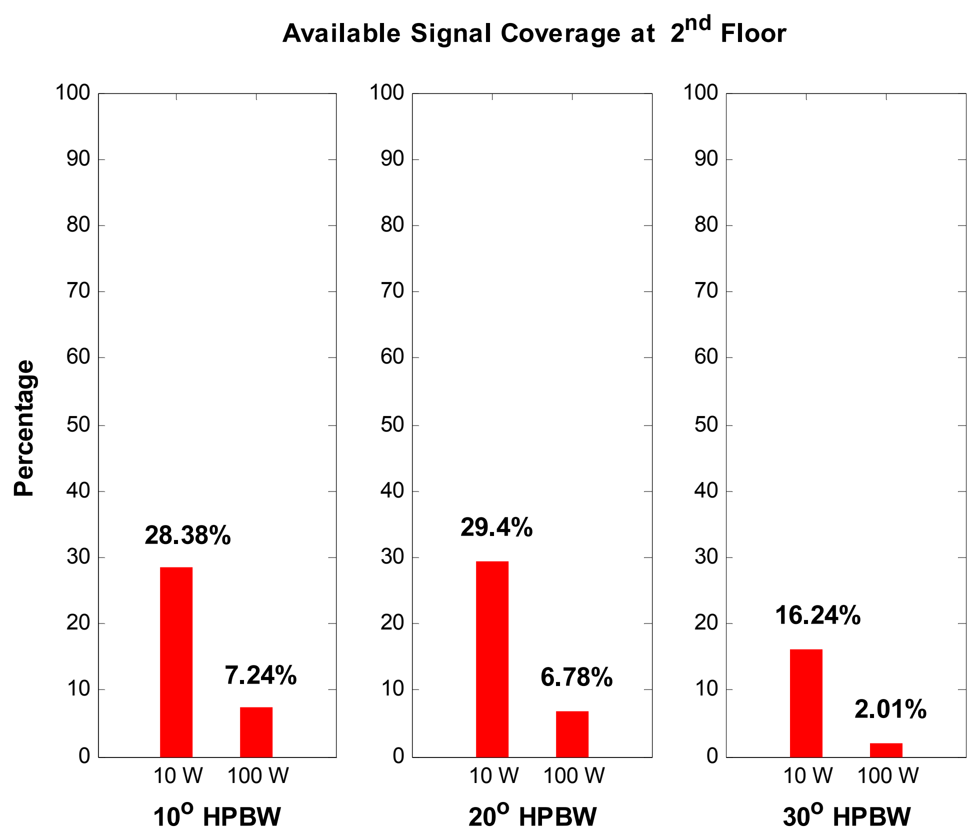

Figure 41. The effects of different HPBWs and power levels for the second floor

Floor	Jammer		Power Difference (dB)		# of Points		Available Signal in the Area
	HPBW	Power (W)	Min	Max	(-) Side	(+) Side	
3	10°	10	-77.56	49.34	1737	1994	53.44%
		100	-87.56	39.34	2807	924	24.77%
	20°	10	-79.63	59.08	1825	1906	51.09%
		100	-89.63	49.08	2975	756	20.26%
	30°	10	-83.07	37.95	2697	1034	27.71%
		100	-93.07	27.95	3464	267	7.16%

Table 14. The results of the *f2fd* command for the third floor

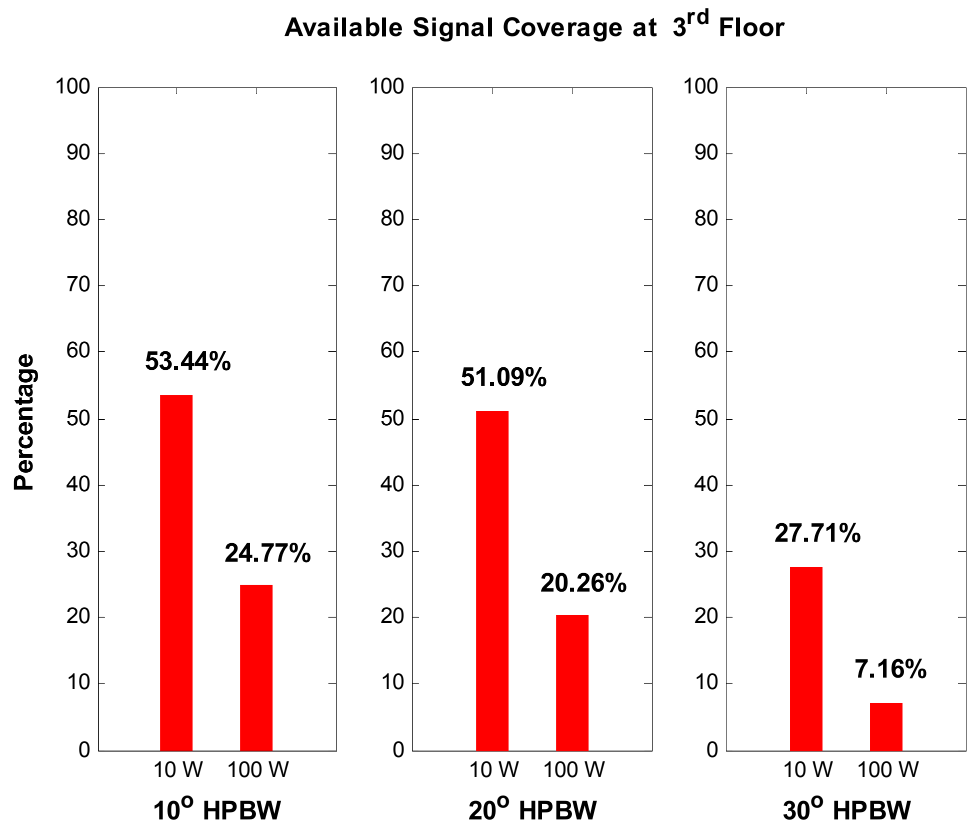

Figure 42. The effects of different HPBWs and power levels for the third floor

Floor	Jammer		Power Difference (dB)		# of Points		Available Signal in the Area
	HPBW	Power (W)	Min	Max	(-) Side	(+) Side	
4	10°	10	-80.01	127.05	1563	2168	58.11%
		100	-90.01	127.05	2599	1132	30.34%
	20°	10	-83.96	127.05	1768	1963	52.61%
		100	-93.96	127.05	2896	835	22.38%
	30°	10	-85.00	127.05	2339	1392	37.31%
		100	-95.00	127.05	3300	431	11.55%

Table 15. The results of the *f2fd* command for the fourth floor

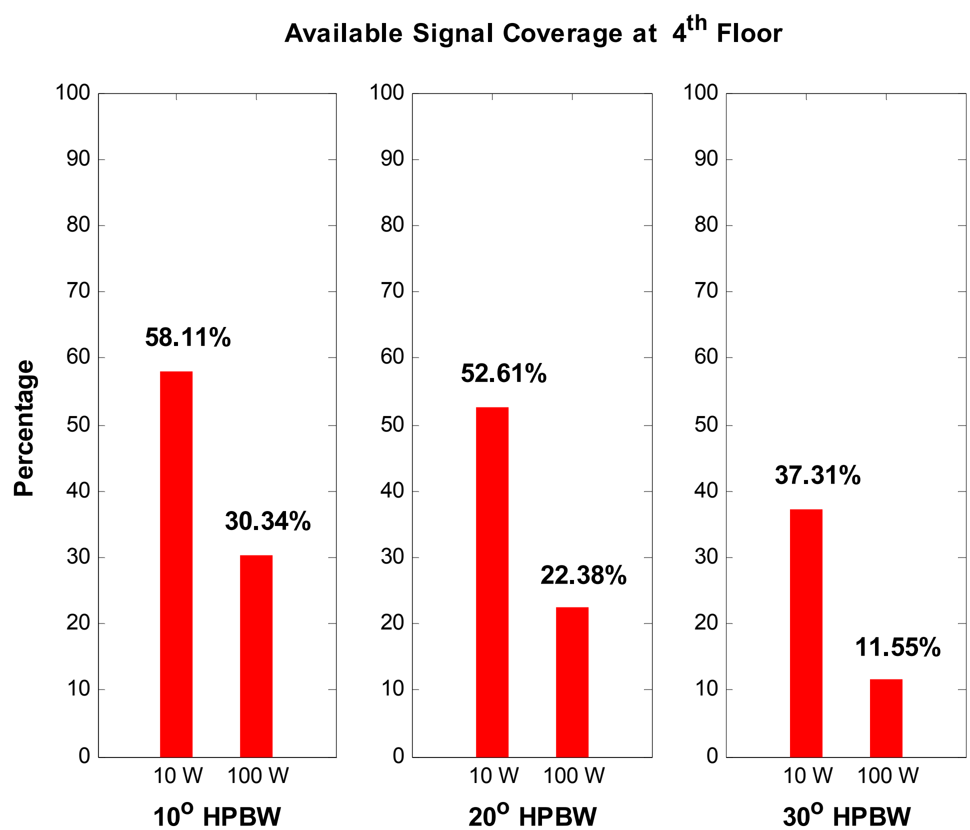

Figure 43. The effects of different HPBWs and power levels for the fourth floor

Floor	Jammer		Power Difference (dB)		# of Points		Available Signal in the Area
	HPBW	Power (W)	Min	Max	(-) Side	(+) Side	
6	10°	10	-123.97	128.52	1545	2186	58.59%
		100	-133.97	128.52	2543	1188	31.84%
	20°	10	-121.61	128.52	1833	1898	50.87%
		100	-131.61	128.52	2903	828	22.19%
	30°	10	-127.20	128.52	2122	1609	43.12%
		100	-137.20	128.52	3122	609	16.32%

Table 16. The results of the *f2fd* command for the sixth floor

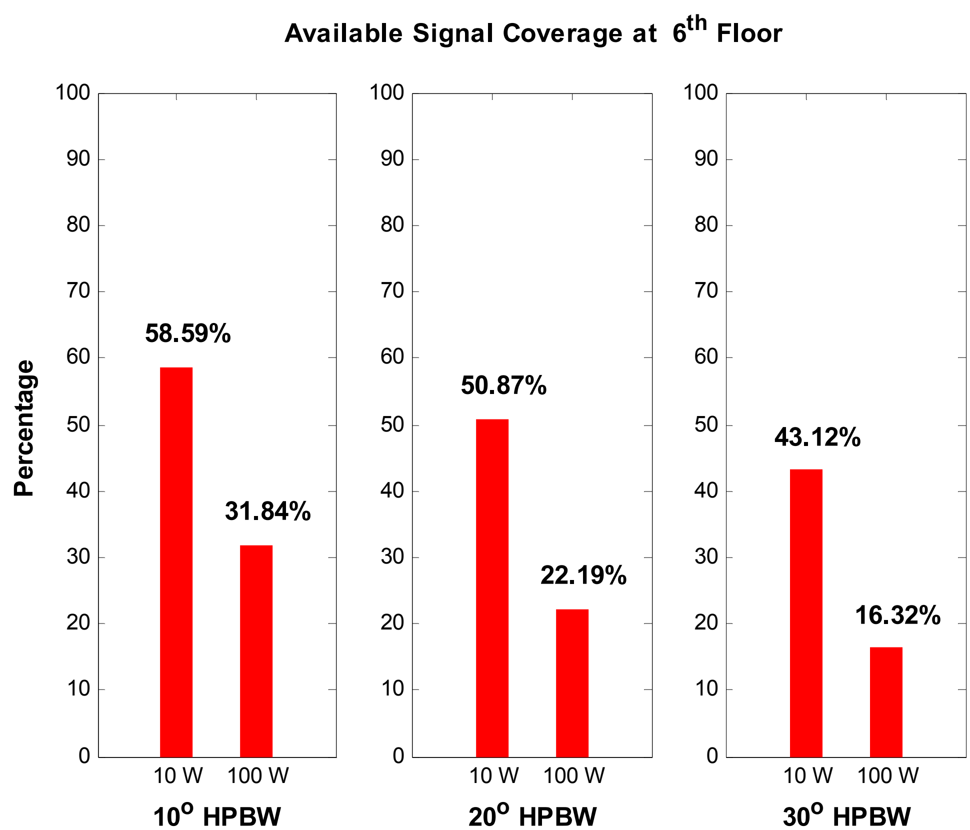

Figure 44. The effects of different HPBWs and power levels for the sixth floor

Floor	Jammer		Power Difference (dB)		# of Points		Available Signal in the Area
	HPBW	Power (W)	Min	Max	(-) Side	(+) Side	
7	10°	10	-113.61	127.84	2094	1637	43.88%
		100	-123.61	127.84	3137	594	15.92%
	20°	10	-117.04	127.84	2497	1234	33.07%
		100	-127.4	127.84	3416	315	8.44%
	30°	10	-119.49	127.84	2640	1091	29.24%
		100	-129.49	127.84	3562	169	4.53%

Table 17. The results of the *f2fd* command for the seventh floor

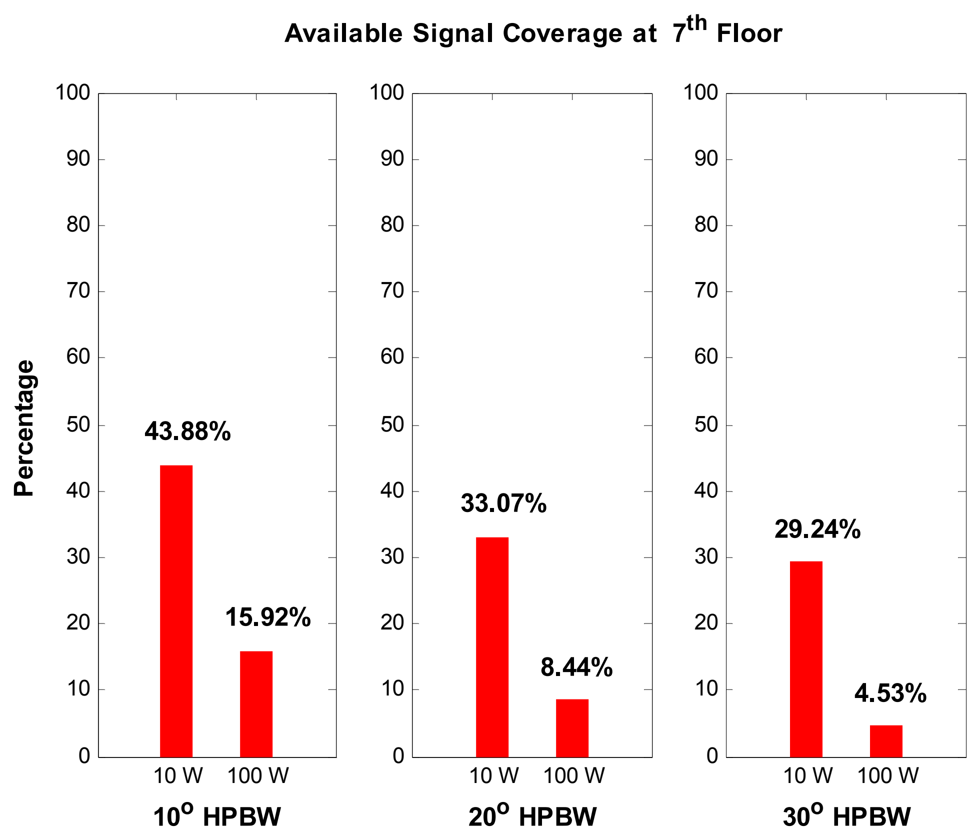

Figure 45. The effects of different HPBWs and power levels for the seventh floor

Floor	Jammer		Power Difference (dB)		# of Points		Available Signal in the Area
	HPBW	Power (W)	Min	Max	(-) Side	(+) Side	
8	10°	10	-120.16	139.07	2799	932	24.98%
		100	-130.16	139.07	3471	260	6.97%
	20°	10	-122.50	139.07	3160	571	15.30%
		100	-132.50	139.07	3590	141	3.78%
	30°	10	-130.26	139.07	3317	414	11.10%
		100	-140.26	139.07	3700	31	0.83%

Table 18. The results of the *f2fd* command for the eighth floor

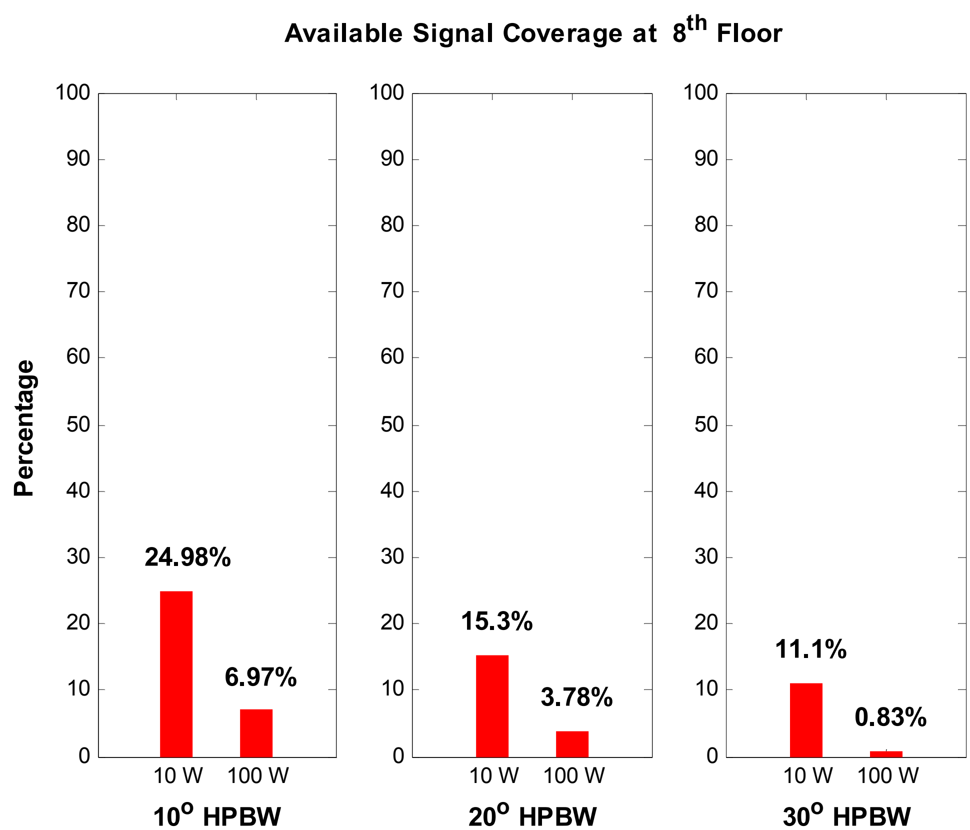

Figure 46. The effects of different HPBWs and power levels for the eighth floor

Floor	Jammer		Power Difference (dB)		# of Points		Available Signal in the Area
	HPBW	Power (W)	Min	Max	(-) Side	(+) Side	
9	10°	10	-187.73	140.11	3218	513	13.75%
		100	-197.73	140.11	3671	60	1.61%
	20°	10	-184.42	140.11	3470	261	7.00%
		100	-194.42	140.11	3690	41	1.10%
	30°	10	-195.19	140.11	3609	122	3.27%
		100	-205.19	140.11	3727	4	0.11%

Table 19. The results of the *f2fd* command for the ninth floor

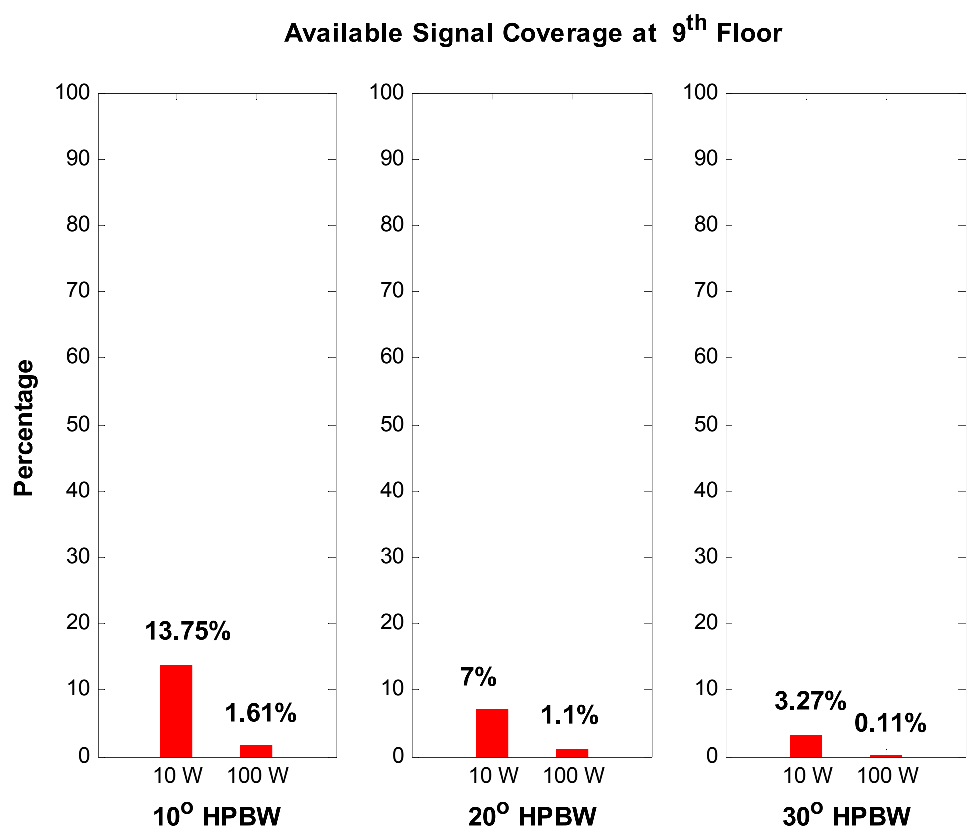

Figure 47. The effects of different HPBWs and power levels for the ninth floor

Floor	Jammer		Power Difference (dB)		# of Points		Available Signal in the Area
	HPBW	Power (W)	Min	Max	(-) Side	(+) Side	
10	10°	10	-193.85	109.44	3629	102	2.73%
		100	-203.85	109.44	3707	24	0.64%
	20°	10	-184.47	109.44	3638	93	2.49%
		100	-194.97	109.44	3707	24	0.64%
	30°	10	-200.72	109.44	3691	40	1.07%
		100	-210.72	109.44	3722	9	0.24%

Table 20. The results of the *f2fd* command for the tenth floor

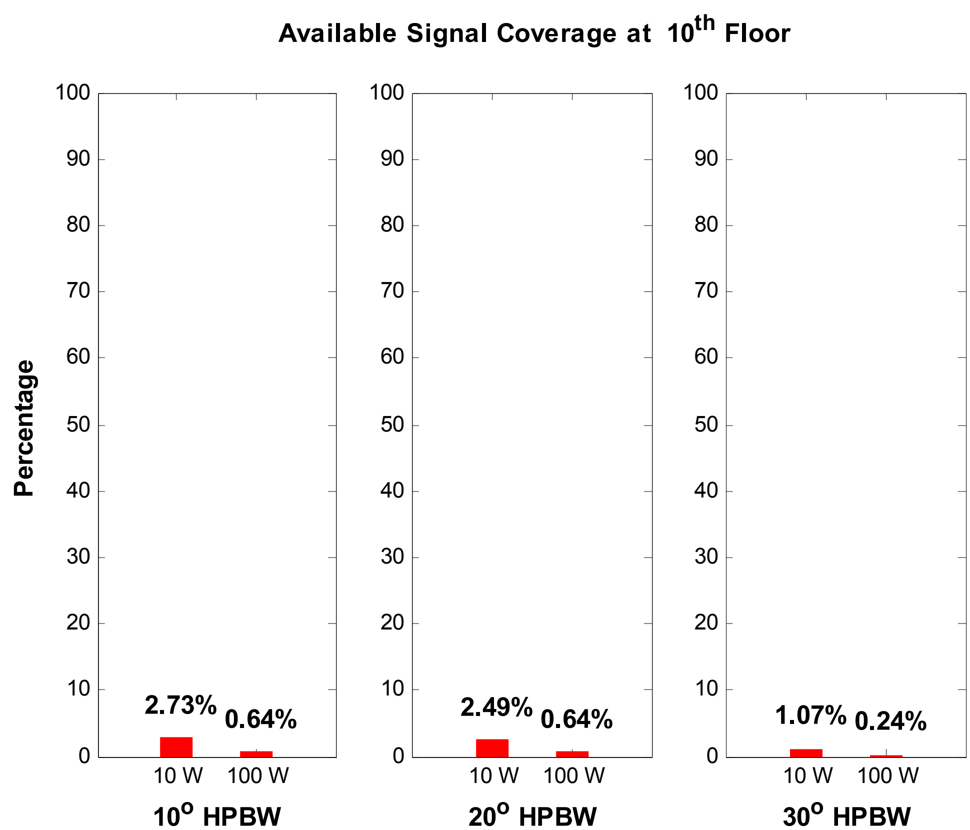

Figure 48. The effects of different HPBWs and power levels for the tenth floor

THIS PAGE INTENTIONALLY LEFT BLANK

LIST OF REFERENCES

[1] "Wireless LAN Security White Paper," http://www.cisco.com/en/US/netsol/ns339/ns395/ns176/ns178/networking_solutions_white_paper09186a00800b469f.shtml, last accessed August 2005.

[2] "Cisco Aironet Wireless LAN Security Overview," http://www.cisco.com/en/US/netsol/ns340/ns394/ns348/ns337/netbr09186a00801f7d0b.html, last accessed August 2005.

[3] "SAFE: Wireless LAN Security in Depth-version 2," http://www.cisco.com/en/US/products/hw/wireless/ps430/products_white_paper09186a008009c8b3.shtml, last accessed August 2005.

[4] P. P. Sumagasay, "Vulnerability of WLANs to Interception," Master's Thesis, Naval Postgraduate School, Monterey, California, September 2002.

[5] Lotfi Boukraa, "Simulation of Wireless Propagation in a High-Rise Building," Master's Thesis, Naval Postgraduate School, Monterey, California, December 2004.

[6] "FCC Rules and Regulations," http://www.fcc.gov/searchtools.html#rules, last accessed August 2005.

[7] T. Rappaport, *Wireless Communications*, Prentice Hall PTR, New Jersey, 2002.

[8] K. Siwiak, *Radiowave Propagation and Antennas for Personal Communications,* 2nd edition, Artech House, Inc., Norwood, Massachusetts, 1998.

[9] E. Hecht, *Optics,* 4th edition, Addison Wesley, San Francisco, California, 2002.

[10] F. T. Ulaby, *Fundamentals of Applied Electromagnetics,* Prentice Hall Upper Saddle River, New Jersey, 2004.

[11] W. L. Stutzman and G.A. Thiele, *Antenna Theory and Design*, 2nd edition, John Wiley & Sons, Inc., Hoboken, New Jersey, 1998.

[12] M. I. Skolnik, *Introduction to Radar Systems,* 3rd edition., McGraw-Hill Companies, Inc., New York, New York, 2001.

[13] D. L. Adamy, *A First Course in Electronic Warfare*, Artech House, Inc., Norwood, Massachusetts, 2001.

[14] D. L. Adamy, *A Second Course in Electronic Warfare,* Horizon House Publications, Inc., 2004.

[15] D. C. Schleher, *Introduction to Electronic Warfare*, Artech House, Inc., Norwood, Massachusetts, 1997.

[16] "Urbana Wireless Toolset," Science Application International Corporation (SAIC), October 2004.

[17] "Urbana 3-D Wireless Toolkit," http://www.saic.com/products/software/urbana/, last accessed August 2005.

[18] Rhinoceros 2.0, http://www.rhino3d.com/whatnew2.htm, last accessed August 2005.

[19] D. C. Jenn, Lecture Notes for EC3630, Radio Wave Propagation, available at www.nps.navy.mil/jenn/EC3630list.html, last accessed May 2005.

[20] A. Chaabane, "Propagation Modeling of Wireless Systems in Shipboard Compartments," Master's Thesis, Naval Postgraduate School, Monterey, California, March 2005.

[21] "Cisco Aironet 802.11a/b/g Wireless PCI Adapter," http://www.cisco.com/en/US/products/hw/wireless/ps4555/products_data_sheet09186a00801ebc33.html, last accessed August 2005.

INITIAL DISTRIBUTION LIST

1. Defense Technical Information Center
   Ft. Belvoir, Virginia

2. Dudley Knox Library
   Naval Postgraduate School
   Monterey, California

3. Chairman
   Department of Information Sciences
   Naval Postgraduate School
   Monterey, California

4. Professor David C. Jenn
   Department of Electrical and Computer Engineering
   Naval Postgraduate School
   Monterey, California

5. Professor Daniel C. Schleher
   Department of Information Sciences
   Naval Postgraduate School
   Monterey, California